PNAS RESEARCH ARTICLE | NEUROSCIENCE
PSYCHOLOGICAL AND COGNITIVE SCIENCES

Goal-directed modulation of the default network supports interactions between selective attention, working memory, and prior knowledge

Veronica Diveica[a,1], Roni Setton[b], Gary R. Turner[c], and R. Nathan Spreng[a,d,e,f,1]

Affiliations are included on p. 11.

Edited by Winrich A. Freiwald, The Rockefeller University, New York, NY; received February 19, 2026; accepted June 5, 2026 by Editorial Board Member Peter L. Strick

Memory is central to flexible, goal-directed behavior. Prior knowledge shapes our current decisions and future plans and guides our attention to selectively prioritize relevant information in our complex, noisy world. Yet, most research on the neural basis of selective attention has focused on novel stimuli and has defined goal relevance based on perceptual features rather than prior knowledge. We investigated how the brain supports selective attention when goal relevance depends on prior knowledge, and compared selection of novel (memory-independent) versus familiar (memory-enhanced) stimuli. Using multiecho fMRI, we recorded brain activity during a selective working memory task involving pictures of famous (familiar) and anonymous (novel) people and places. We manipulated the relevance of fame to task performance: In "fame relevant" task blocks, participants selectively attended to famous while ignoring anonymous stimuli; in "fame irrelevant" blocks, they attended to anonymous while ignoring famous stimuli. Compared to a nonselective, categorization task, the selective working memory task elicited sustained coactivation of frontoparietal control and dorsal attention networks. Task-relevant contrasted with task-irrelevant stimuli elicited transient coactivation of frontoparietal control and default network regions, irrespective of stimulus fame. Within the DN, this effect was driven by both enhanced activation for task-relevant stimuli and suppression for task-irrelevant stimuli, confirming attention-driven neuromodulation. Further, selective working memory coactivated these high-order, heteromodal brain networks while lowering activity in visual regions. Our findings elucidate the neural underpinnings of prior knowledge-guided selection of perceptual inputs for working memory, suggesting differences from those previously reported for perception-guided selection.

attention | cognitive control | working memory | semantic knowledge | multiecho fMRI

Significance

As humans go about their lives, they experience a continuous stream of novel and familiar stimuli, not all of which are relevant to current goals. Prior knowledge plays a crucial role in evaluating stimulus relevance. We investigated how the brain facilitates goal-directed selective attention to relevant stimuli while filtering out distractors when relevance is determined by prior knowledge. Our results show that this ability relies on coactivation of the frontoparietal control and default networks, alongside suppression of the visual network. These findings highlight how the brain enables the control of attention based on prior knowledge and indicate that the underlying neural pathways may differ from those engaged when selection is guided by perception.

The ability to selectively attend to relevant information while ignoring distractors is crucial for goal-directed cognition, enabling efficient allocation of limited cognitive resources. The goal relevance of incoming information can be determined by perceptual features or through associations with prior knowledge. We rely on both perception and memory to filter the myriad information streams that confront us. Imagine conversing with a friend about a common acquaintance when it jogs a memory about the acquaintance's recent health scare. Your attention shifts from the immediate perceptual milieu (the current conversation) to remember whether the acquaintance had given you permission to disclose, before you return to the conversation. In this simple example, actively moving attention from the external perceptual environment to internal memory representations (and back) was critically necessary to the goal of sustaining a fluid social exchange, without compromising a friend's confidence. Goal-directed shifting of attention from perception to memory is common in our everyday lives. Despite this, the vast majority of cognitive neuroscience research on selective attention has focused on perceptually guided selection, largely to the exclusion of selection dependent on prior knowledge.

Here, we use "selective attention" to refer to the selection and prioritization of goal-relevant information for processing, and the inhibition of goal-irrelevant information (1–3). Selective attention is commonly investigated using paradigms in which attention is guided toward specific spatial locations (spatial attention), perceptual features (e.g., color; feature-based attention), or objects (object-based attention) among competing alternatives (3–5). It has also been studied using paradigms requiring selective encoding of goal-relevant perceptual inputs in working memory while ignoring distractors, where goal relevance is determined by perceptual information such as stimulus category (6). We refer to these operationalizations collectively as perceptually guided selective attention. Furthermore, prior work has predominantly used novel stimuli without strong prior knowledge associations (e.g., geometric

Author contributions: V.D., R.S., G.R.T., and R.N.S. designed research; V.D., R.S., G.R.T., and R.N.S. performed research; V.D. analyzed data; V.D. and R.S. curated data; V.D., G.R.T., and R.N.S. acquired funding; R.N.S. supervised the research; V.D. wrote the paper; and V.D., R.S., G.R.T., and R.N.S. reviewed and edited the paper.

The authors declare no competing interest.

This article is a PNAS Direct Submission. W.A.F. is a guest editor invited by the Editorial Board.

[1]To whom correspondence may be addressed. Email: veronica.diveica@mcgill.ca or nathan.spreng@mcgill.ca.

This article contains supporting information online at https://www.pnas.org/lookup/suppl/doi:10.1073/pnas.2605179123/-/DCSupplemental.

Published July 13, 2026.

shapes). This work has revealed that perceptually guided selective attention relies on a top–down modulatory mechanism, in which signals from prefrontal and parietal cortices enhance activity in perceptual regions that process goal-relevant perceptual information while suppressing activity in those perceptual regions with preferential selectivity for irrelevant information (1–4). Top–down attentional modulation targets different perceptual regions depending on the type of attention: Spatial attention modulates retinotopically organized early and extrastriate visual areas (7); feature-based attention modulates feature-selective regions such as V4 and MT (8, 9); object-based attention modulates category-selective cortices (10) and distributed representational patterns across higher-level ventral visual areas (11). The sources of top–down neuromodulation include the inferior frontal junction, middle frontal gyrus, anterior inferior parietal lobule and part of the intraparietal sulcus (12–14), which are affiliated with the frontoparietal control network (FPCN; Fig. 3*E*) (15, 16). The frontal eye fields, the posterior superior parietal cortex, and part of the intraparietal sulcus, which comprise the dorsal attention network (DAN) (16, 17) have also been implicated (18–20). The DAN contains topographic maps of visual space and is essential for externally focused, goal-directed spatial orientation of attention (7, 21). The FPCN represents abstract rules, goals, and context (22, 23) and modulates lower-level processes via flexible, context-dependent functional connectivity (FC) with more domain specific and specialized processing regions or networks (24, 25).

The FPCN has also been implicated in the interaction between attention and memory, particularly in visuospatial orientation of attention guided by episodic memory representations (26, 27), selection between items maintained in working memory (28), and shifts of attention between the external environment and internally oriented states such as working memory content and mind-wandering (29, 30). However, its role in goal-directed prioritization versus inhibition of perceptual inputs for further working memory processing when relevance is determined by prior knowledge (e.g., familiarity with a person) has yet to be directly investigated.

Access to prior knowledge is underpinned by a set of frontal, temporal, and parietal brain areas collectively known as the default network (DN) (31–33). Neuropsychological and neuroimaging investigations have revealed that the hippocampus is necessary for the formation and retrieval of episodic memories (34), while the anterior temporal lobe is crucial for accessing semantic knowledge (35). Tasks that require episodic, semantic, or autobiographical memory retrieval also elicit overlapping activation in other DN regions, including the inferior frontal gyrus, lateral temporal cortex, inferior parietal lobe, medial prefrontal cortex, and retrosplenial and posterior cingulate cortices (31, 36, 37). Given this functional affiliation with prior knowledge stored in long-term memory, we reasoned that the DN may play a critical role in selective attention when goal relevance depends on prior knowledge, particularly when the targets of selection are stimuli that are enhanced by such knowledge (e.g., familiar stimuli).

DN activation is consistently observed during memory-based, social, and introspective tasks (38, 39), suggesting a key role in cognitive states that rely primarily on internally generated, or perceptually decoupled, information. This includes decisions guided by working memory contents rather than immediately available perceptual input (40–42). The DN's position at the apex of a unimodal-to-heteromodal gradient of macroscale functional organization, also known as the principal gradient (43), may reflect its role in perceptually decoupled thought, as its functional and physical distance from sensory cortices may insulate DN regions from perceptual control, facilitating internally oriented cognition (44, 45). Furthermore, the comparable positions of the DN and FPCN at the heteromodal apex of this gradient indicate that their FC profiles are highly similar, suggesting a propensity for functional cooperation and task-driven coactivation (46). Consistent with this idea, several studies have now reported coactivation of FPCN and DN during cognitive control tasks that require access to prior knowledge (47–50). These findings raise the possibility that the FPCN may collaborate with the DN to support selective attention when selection involves DN-mediated memory processes, but this has received limited empirical attention.

Here, we investigated the neural correlates of selective attention when the goal relevance of perceptual inputs depends on prior knowledge associations, rather than on perceptual information. Specifically, we focused on the selection and prioritization of stimuli for working memory in the face of distractors, a type of selective attention that has been less studied than feature-based or spatial attention. We tested whether this form of selection relies on similar top–down control mechanisms as perceptually guided selective attention, involving coactivation of frontoparietal control and sensory regions (24), or whether it instead engages DN regions, and FPCN-DN coactivation. We further tested whether the modulation of DN activation by selective attention is specific to stimuli associated with prior knowledge, but not unfamiliar stimuli, in line with its role in prior knowledge representation.

To address these questions, we collected multiecho fMRI data while participants performed a selective working memory (N-back) task in which goal relevance depended on prior knowledge, and the stimuli were either associated with long-term memory representations (memory-enhanced) or not (memory-independent) (Fig. 1*B*). In brief, stimuli (faces or places) were presented on a trial-wise basis, and participants judged whether the current image matched an image presented "n" trials back (Fig. 1*A* and *Materials and Methods*). Stimuli were either famous, engaging memory-enhanced representations, or anonymous, engaging memory-independent representations. Critically, selective attention was manipulated at the block level by instructing participants to attend to either famous or anonymous stimuli, while ignoring the other. Task-relevance was signaled by the presence of prior knowledge associations in "fame relevant" blocks and their absence in "fame irrelevant" blocks. Consequently, evaluating stimulus relevance required access to long-term memory. To successfully complete the task, participants needed to evaluate the relevance of each stimulus, but select only task-relevant stimuli for working memory processing, while inhibiting irrelevant stimuli. Consequently, the contrast between task-relevant and irrelevant trials reflects prioritization of working memory—specifically, comparing perceptual input with working memory representations to identify matches, and retaining perceptual input in working memory for subsequent goal-directed use—relative to the suppression of such processing. This contrast reflects processes that go beyond input–output mapping and are distinct from feature-based and spatial attention. This design also allowed us to directly contrast attentional selection of memory-enhanced (famous) with memory-independent (anonymous) stimulus representations. To disambiguate the brain responses specific to top–down control versus lower-level processes, participants also completed a categorization control task that did not require selective attention or working memory.

Given the DN's role in accessing working memory representations in the service of goal-directed cognition (40–42, 47), we hypothesized that the DN would coactivate with frontoparietal control regions during task-relevant versus irrelevant trials. In light of the DN's established role in long-term memory (37, 51), we hypothesized that the modulation of DN activity by task relevance would be stronger for famous relative to anonymous stimuli. Because these large-scale networks are functionally heterogeneous (38, 52), we further expected that distinct activation patterns may arise across known DN and FPCN subnetworks (53). We hypothesized that effects of task relevance would reflect context-dependent enhancement *and* suppression

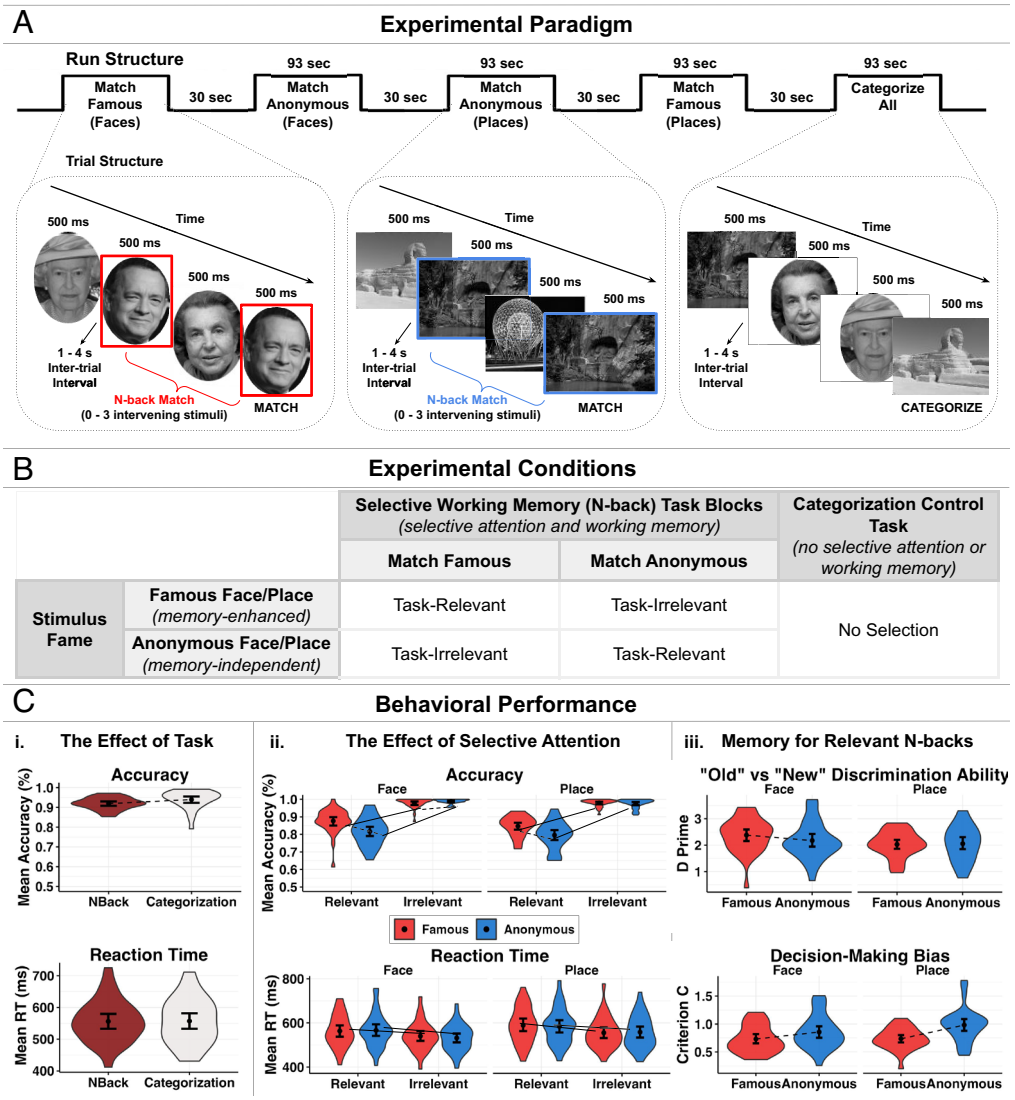

Fig. 1. Overview of the Study Design and Behavioral Performance. (*A*) The experimental paradigm used a mixed block/event-related design with separate blocks for each task interleaved with fixation periods. N-back task blocks featured streams of trials involving famous and anonymous faces or places, with N-back matches separated by a variable number of stimuli (0 to 3). The categorization block included interleaved famous and anonymous face and place trials. (*B*) Experimental conditions and their relationship to the cognitive processes under investigation, illustrating how stimulus fame interacts with the selective working memory task block to determine trial task-relevance. (*C*) The figures display the distributions of behavioral indices, means, and 95% CIs. Connecting lines between means highlight statistically significant differences between conditions. i) Mean participant accuracy and RT (on correct trials only) as a function of task (N-back vs Categorization); ii) Mean participant accuracy and RT (on correct trials only) for N-back trials as a function of task relevance, fame, and domain. Dashed lines highlight statistically significant differences between fame conditions, and solid lines highlight significant differences between task relevance conditions. iii) Memory for relevant N-back trials as a function of fame and domain. D prime quantifies the ability to discriminate between "old" (i.e., repeat) vs "new" stimuli. Criterion C quantifies response bias, with lower values suggesting a higher tendency to report that a stimulus had been previously seen (i.e., it is a repeat trial). Note: The behavioral analyses on accuracy and RTs were conducted on individual trial-level data, but aggregate metrics are displayed for ease of visual interpretation.

of regional activation magnitude, consistent with established models of top–down neuromodulation (10). Finally, we predicted that the selective working memory task would shape whole-brain activation patterns along the macroscale principal connectivity gradient, demonstrating recruitment of the heteromodal end and, thus, reliance on a perceptually decoupled brain state.

Results

We investigated the brain activity underpinning selective attention to famous (memory-enhanced) versus anonymous (memory-independent) stimuli within an N-back selective working memory task where stimulus relevance (relevant vs. irrelevant) was manipulated based on prior knowledge (famous vs. anonymous) across two stimulus domains (faces vs. places). We first present our behavioral findings before presenting the results of the brain activation analyses.

Behavioral Performance Is Modulated by Task, Stimulus Relevance, and Prior Knowledge. As expected, performance was worse during the selective working memory conditions versus the categorization control task. Participants provided more accurate responses on categorization versus N-back trials (Fig. 1*C*; Odds Ratio = 0.7, SE = 0.055, z = −6.3, $P < 0.001$). There was no effect of task condition on reaction times (RTs) during accurate trials (std. β = −0.0045, SE = 0.013, z = −0.36, $P = 0.72$).

Based on previous findings, we predicted that N-back performance would be enhanced for famous (memory-enhanced) versus anonymous (memory-independent) stimuli as long-term memory associations have been shown to improve working memory performance (47, 54, 55). To ensure participants had prior knowledge of the famous faces and places, only stimuli that were correctly recognized as famous in a postscan manipulation check were included in the following behavioral analyses. Performance was more accurate on famous than anonymous faces and places during goal-relevant trials (Fig. 1*C*; Faces: marginal means difference (MMD) = 0.53, SE = 0.15, $P < 0.001$; Places: MMD = 0.38, SE = 0.14, $P = 0.0085$). In contrast, performance was less accurate on famous versus anonymous face trials when fame was goal-irrelevant (i.e., distracting) (MMD = −0.51, SE = 0.22, $P = 0.019$), although this effect was not observed for places (MMD = 0.18, SE = 0.2, $P = 0.35$). These results demonstrate that access to prior knowledge can both support and hinder task performance depending on the goal-relevance of that prior knowledge. No significant effect of fame was observed on RTs during correct trials (Table 1).

To further interrogate the effect of fame on working memory performance, we modeled participants' responses during goal-relevant N-back trials using signal detection metrics (56) (Fig. 1*C*). Participants showed better memory discrimination (higher *d* prime) between novel and repeat (match) stimuli for famous versus

Table 1. Summary of statistical results from behavioral analyses

Behavior	Predictor	Estimate	SE	t	*P*
Accuracy	Fame	1.16	0.11	1.34	0.18
	Task Relevance	0.09	0.07	−37.09	<0.001***
	Domain	1.33	0.11	2.62	0.01**
	Fame * Task Relevance	1.86	0.13	4.73	<0.001***
	Fame * Domain	0.76	0.22	−1.25	0.21
	Task Relevance * Domain	0.91	0.13	−0.73	0.46
	Fame * Task Relevance * Domain	2.32	0.26	3.22	<0.001***
RT	Fame	0.01	0.02	0.26	0.79
	Task Relevance	0.21	0.01	16.87	<0.001***
	Domain	−0.14	0.02	−6.88	<0.001***
	Fame * Task Relevance	−0.02	0.02	−0.71	0.48
	Fame * Domain	0.02	0.04	0.46	0.64
	Task Relevance * Domain	−0.01	0.02	−0.55	0.58
	Fame * Task Relevance * Domain	−0.11	0.05	−2.31	0.02*
D Prime	Fame	0.14	0.12	1.17	0.25
	Domain	0.37	0.1	3.66	<0.001***
	Fame * Domain	0.37	0.18	2.01	0.05*
Criterion C	Fame	−0.66	0.13	−4.95	<0.001***
	Domain	−0.23	0.13	−1.73	0.09
	Fame * Domain	0.43	0.27	1.6	0.11

Note. Estimates represent Odds Ratios for the Accuracy analysis and regression beta coefficients for the RTs, D Prime and Criterion C analyses. RT = reaction times, SE = the SE of the estimate of interest (either Odds Rations or beta coefficients).

anonymous faces (MMD = 0.21, SE = 0.1, $P = 0.036$). This fame effect was only trending for places (MMD = −0.03, SE = 0.1, $P = 0.077$). Participants were generally cautious about reporting stimuli as previously seen (Criterion C > 0); however, this conservative response bias was reduced for famous compared to anonymous faces and places (lower Criterion C; Table 1). These results show that prior knowledge improves working memory performance while also biasing response strategy to reduce misses, at the risk of incorrectly endorsing novel famous stimuli as N-back matches.

Patterns of Brain Activity are Modulated by Task, Stimulus Domain, and Prior Knowledge. To confirm whether our core manipulations were effective in altering brain responses, we first examined whether patterns of BOLD activity differed based on task (N-back vs. Categorize) and stimulus domain (faces versus places). To this end, we used partial least squares (PLS), a data-driven multivariate analysis (57, 58) that can detect whole-brain patterns of task-related coactivation. A significant pattern of brain activity dissociated the two tasks ($P < 0.001$; Fig. 2*B* and *SI Appendix*, Table S1). Sustained N-back task performance over the block was associated with increased BOLD signal in regions overlapping significantly with the FPCN and DAN (Fig. 2*C*), as quantified using the dice coefficient and spin permutation significance testing (cf., (59). These regions included the presupplementary motor area, precuneus, middle frontal gyri, bilateral anterior insula, intraparietal sulci, and the right inferior/middle temporal gyrus (Fig. 2*A*). Conversely, Categorization task performance was associated with activation of a distinct set of regions including the cingulate cortex, left pre- and postcentral gyri, bilateral posterior insula, and fusiform gyri. Next, we examined sustained activity associated with working memory for faces versus places. A significant pattern of activity dissociated face from place N-back blocks ($P < 0.001$; Fig. 2*F* and *SI Appendix*, Table S2). Consistent with previous research, we found that faces elicited peak activation in the right posterior fusiform gyrus (Fig. 2*E*), referred to as the fusiform face area due to its selective response to faces (60). Conversely, places were associated with peak activation in the left parahippocampal gyrus, referred to as the putative parahippocampal place area due to its selective response to scenes (61).

To test our prediction of DN involvement during access to prior knowledge, we next examined transient activity associated with processing a famous relative to an anonymous stimulus. To ensure participants had prior knowledge of the famous faces/places, only stimuli correctly rated as famous in a postscan manipulation check were considered in this analysis, as well as the analyses reported below. Moreover, to control for any recent memory effects, we analyzed only the first occurrence of each specific face or place during the experimental session. A significant pattern of activity dissociated famous from anonymous stimuli, irrespective of domain ($P < 0.001$, explaining 48.46% of the covariance; Fig. 2*J* and *SI Appendix*, Table S3). This confirmed that famous faces and places engaged regions that significantly overlap with the DN (Fig. 2*K*), including medial prefrontal cortex, precuneus, left middle temporal gyrus, and angular gyri (Fig. 2*I*). In contrast, anonymous faces and places were associated with regions largely overlapping with the visual network and DAN, including bilateral occipital cortex, supplementary motor area, and middle frontal gyrus. In line with previous research showing preferential DN engagement by social compared to nonsocial information (62, 63), the fame-related activation pattern was expressed more strongly for faces than for places.

To aid interpretation of the whole-brain covariance patterns, we show BOLD signal magnitude differences relative to block/trial onsets from regions exhibiting reliable task-related covariance (Fig. 2 *D*, *H*, and *L*), in line with common practices (e.g., 37, 64, 65). These plots are descriptive rather than inferential.

Frontal Parietal Control and Default Network Region Activity Covaries During Selective Attention. Having demonstrated that our core task manipulations were associated with predicted differences in brain responses, next we tested our main prediction that DN activation supports selective working memory. Trials were

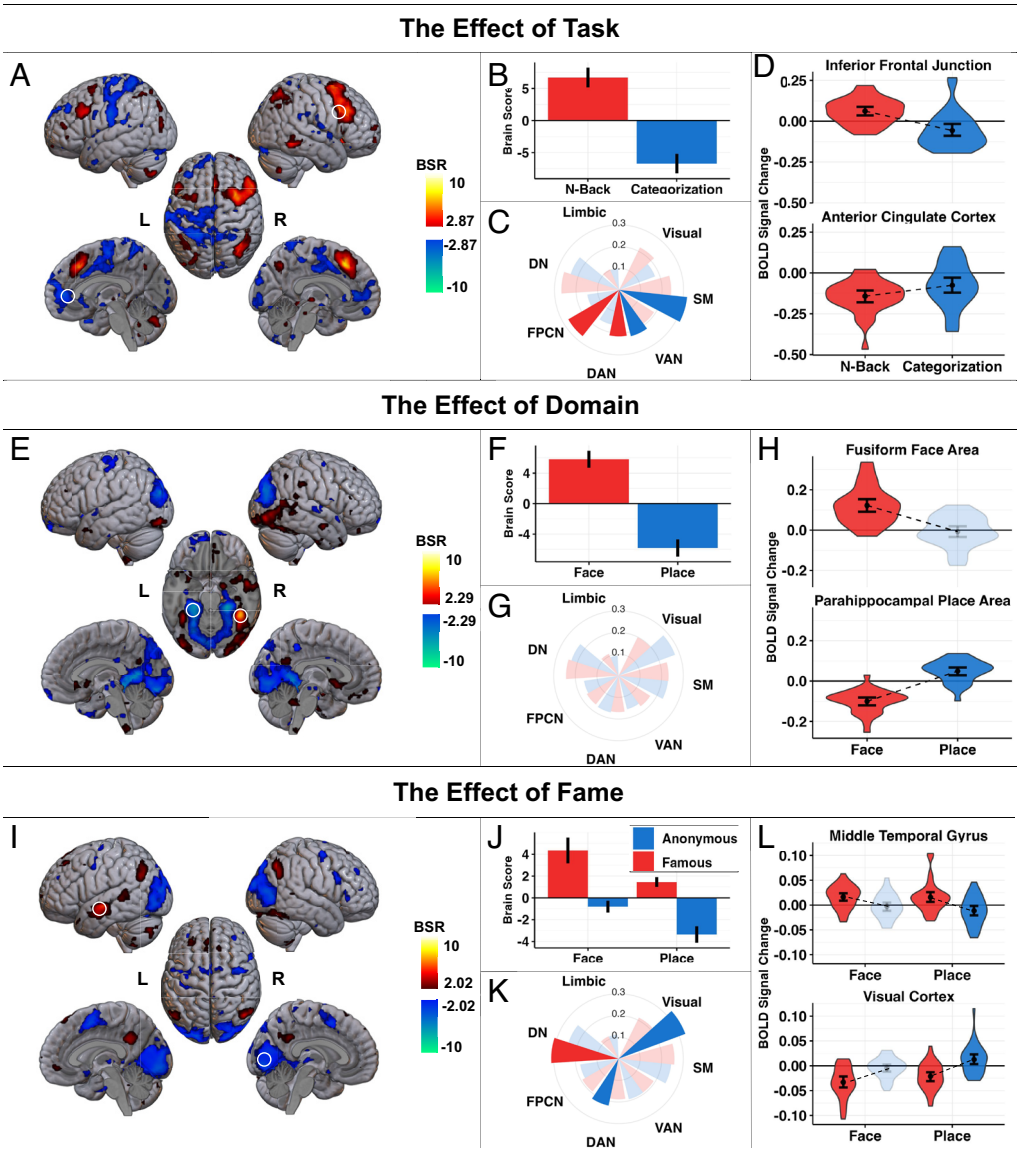

Fig. 2. (*A–D*) Differences in sustained activity during N-back vs Categorization blocks. The maps show the top 5% of voxels based on BSR values (BSR > ± 2.87, equivalent to $P < 0.004$). (*E–H*) Differences in sustained activity during Face vs Place N-back blocks. The maps show the top 5% of voxels based on BSR values (BSR > ± 2.29, $P < 0.022$). (*I–L*) Differences in transient activity evoked by famous compared to anonymous stimuli. The maps show the top 5% of voxels based on BSR values (BSR > ± 2.37, $P < 0.018$). (*B*, *F*, and *J*) The mean brain scores (±SD) associated with the statistically significant LVs. (*C*, *G*, and *K*) The degree of overlap between the brain patterns associated with the positive (red) and negative (blue) expression of the LV (thresholded at |BSR| > 1.96, $P < 0.05$) and the 7-network parcellation from Yeo et al. (53). Solid colors indicate statistically significant overlap, while transparent colors indicate nonsignificant overlap. (*D*, *H*, and *L*) Descriptive plots of the mean BOLD signal change (±95% CIs) relative to trial/block onset in representative regions highlighted by white circles on the corresponding activation maps. The distribution across participants is also displayed—solid colors indicate statistically significant increases/decreases from baseline, while transparent colors indicate the lack of significant changes from baseline. The dashed lines highlight statistically significant differences between conditions. Note. BSR = bootstrap ratio; SM = somatomotor network; VAN = ventral attention network; DAN = dorsal attention network; FPCN = frontoparietal control network; DN = default network; BOLD = blood oxygen level–dependent signal.

collapsed across domain, given our finding that DN is engaged by fame regardless of domain (Fig. 2 *I–K*). Only correct trials and only the first instance a stimulus was task-relevant and irrelevant were considered. There was one significant pattern of activity that covaried with the task conditions. Contrary to predictions, this pattern dissociated relevant from irrelevant stimuli, irrespective of fame ($P < 0.001$; Fig. 3*B* and *SI Appendix*, Table S4). Task-relevant famous and anonymous stimuli elicited activation in extensive regions of frontal, parietal, and temporal cortices (Fig. 3*A*). This activity pattern showed statistically significant overlap with the DN and the FPCN (Fig. 3*C*). Task-irrelevant famous and anonymous stimuli engaged the bilateral occipital cortices, parahippocampal gyrus, presupplementary motor area, and left pre- and postcentral gyri. This activity pattern overlapped significantly only with the visual network. The effect was reliably observed across regions containing topographic maps of visual space and was particularly pronounced in higher-level occipito-temporal regions (*SI Appendix*, Fig. S3*B*).

Next, we conducted a control analysis to examine whether selective attention explained more variance in brain activity patterns than the other task manipulations. We split the trials by task-relevance, fame, and domain, and the main effects of each factor were explicitly modeled in a PLS analysis. Task-relevance was the only significant contrast (*SI Appendix*, Fig. S1*B*), explaining 91.2% of the covariance ($P < 0.001$), whereas fame explained 3.95% ($P = 0.71$) and domain explained 4.84% (p = 0.28). The whole-brain pattern of neural activity (*SI Appendix*, Fig. S1*A*) dissociated task relevant from irrelevant trials irrespective of stimulus fame and domain in this control analysis and was virtually identical to the main data-driven analysis (r = 0.996, spin permutation $P = 0.001$). This demonstrates that the selective attention manipulation, whether a trial was task-relevant or irrelevant, explained more variance in whole brain covariance patterns of BOLD signal than whether it was famous or anonymous or whether it was a face or place.

In a final control analysis, we tested whether the effect of task relevance on brain activity was specific to top–down control, or whether it could be explained by confounding lower-level processes. To address this question, we compared transient activity evoked by relevant and irrelevant N-back trials, with that evoked by categorization trials, which placed greater demands on bottom–up perceptual processing without the need for selective working memory. Only the first instance of a stimulus (when it was task-relevant, irrelevant, or categorized) were considered for analysis. We found a significant pattern of neural activity (*SI Appendix*, Fig. S1*D*) that dissociated relevant from irrelevant trials, regardless of fame, and which was nearly identical to that observed in the main analysis

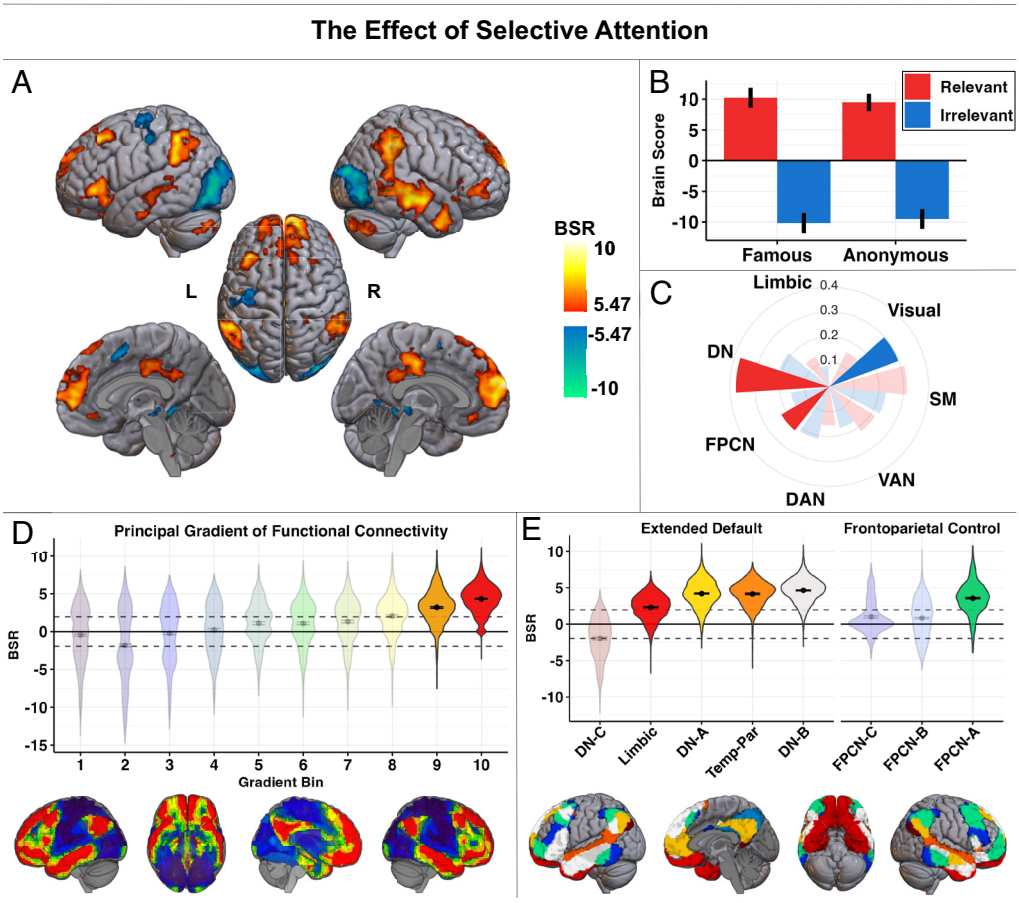

Fig. 3. Differences in the transient activity evoked by Relevant vs Irrelevant famous/anonymous stimuli. (*A*) The whole brain pattern associated with the only significant LV. The maps show the top 5% of voxels based on BSR values (BSR > ± 5.47, equivalent to $P < 4.42e{-}08$). (*B*) The mean brain scores (±SD) associated with the LV, indicating a main effect of task relevance irrespective of fame. (*C*) The degree of overlap between the brain patterns associated the positive (red) and the negative (blue) expression of the LV (thresholded at BSR > 1.96, $P < 0.05$) and the 7-network parcellation from Yeo et al. (53). Solid colors indicate statistically significant overlap, while transparent colors indicate nonsignificant overlap. (*D*) The mean BSR scores (±99% CIs) across the voxels that fall within each bin of the principal gradient from Margulies et al. (43). The distribution of BSR values across all voxels is also displayed—solid colors indicate statistically significant differences from the BSR threshold of reliability, while transparent colors indicate nonsignificant differences. (*E*) The mean BSR scores (±99% CIs) across the voxels that fall within the extended DN and FPCN subnetworks from Yeo et al. (53). The dashed lines indicate BSR = ±1.96 (equivalent to $P = 0.05$). Note. BSR = bootstrap ratio; SomMot = somatomotor network; VAN = ventral attention network; DAN = dorsal attention network; FPCN = frontoparietal control network; DN = default network.

(r = 0.994, spin permutation $P = 0.001$). Notably, categorized anonymous trials covaried with the irrelevant N-back trials but expressed the neural activity pattern to a lesser extent, while categorized famous trials did not align with this activity pattern (*SI Appendix*, Fig. S1*E*). When comparing only task-relevant and categorization trials, a similar overall pattern was observed, but categorization trials showed a response opposite to relevant trials irrespective of fame (*SI Appendix*, *Result* and Fig. S5). These results confirm that DN and FPCN coactivation during the N-back task is not driven by bottom–up processes and is specific to top–down control.

The finding that transient increases in visual cortex activation are negatively related to task-relevant trials may seem counterintuitive. Rather than a lack of activation in response to visual stimuli, this effect reflects relative differences between stimuli selected for further goal-directed processing, and irrelevant stimuli that must be inhibited. In a supplementary analysis (*SI Appendix*, Result and Fig. S2), we confirmed that, compared to fixation only rest blocks, the task blocks elicited sustained activation in both low-level and higher-order visual regions (*SI Appendix*, Fig. S3*A*). Therefore, the transient visual cortex deactivation observed for task-relevant versus irrelevant trials occurs against a background of sustained activation. Furthermore, although we observed opposing activation patterns in frontal control and visual regions during relevant versus irrelevant trials, we found that FC between frontal control and category-selective perceptual cortex supported the maintenance of task-relevant stimuli in working memory, consistent with current models of working memory (66) (*SI Appendix*, Result and Fig. S4).

Frontoparietal Control and Default Network Engagement During Selective Attention Varies Across Subnetworks. Having identified a role for the FPCN and DN in selective working memory, and recognizing that these large-scale networks are functionally heterogeneous (38, 52), we next examined whether and how subnetworks within the FPCN and extended DN (Fig. 3*E*) were reliably modulated by selective attention, enabling more spatially specific network-level inferences. The extended DN includes regions from the default, limbic, and temporoparietal (Temp-Par) subnetworks, as defined by Yeo et al. (53). The inclusion of the Limbic subnetwork is based on its affiliation with the DN in our recent work (67), while Temp-Par regions are affiliated with the DN at coarser resolutions (53) and are consistent with a language network (68). Except for DN-C, all extended DN subnetworks, including DN-A, DN-B, Limbic, and Temp-Par, were reliably engaged by task-relevant compared to task-irrelevant trials (Fig. 3*E* and *SI Appendix*, Table S6). Among the FPCN subnetworks, only FPCN-A showed reliable activation to task-relevant versus irrelevant trials. This is consistent with the FPCN-A's close affiliation with the DN (52). These findings highlight the widespread engagement of the DN, in contrast to the more spatially circumscribed involvement of the FPCN.

Brain Activity in Visual and Default Network Shows Context-Dependent Enhancement and Suppression. Consistent with neuromodulation theories of top–down attentional control (10, 66), neural activity differences between task-relevant and task-irrelevant trials may arise from enhanced activation to relevant trials, suppressed activation to irrelevant trials, or both. Differential enhancement *and* suppression of neural activity in response to relevant and distracting information, relative to baseline activation levels, is a neural signature of successful top–down modulation (10, 69). Therefore, we tested whether DN and visual regions exhibited both enhanced processing of relevant stimuli *and* suppressed processing of irrelevant stimuli relative to the nonselective perceptual processing during the categorization

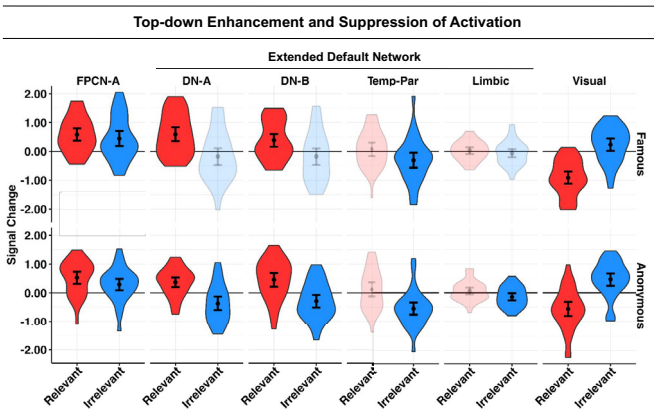

Fig. 4. Top–down enhancement and suppression of the magnitude of activation in the extended DN, FPCN-A, and Visual networks. Mean standardized t scores (±95% CIs) for the contrast between selective working memory task trials and categorization baseline trials, as a function of task relevance and fame. Solid colors indicate statistically significant increases/decreases relative to the categorization baseline, while transparent colors indicate nonsignificant changes.

trials. Enhancement was indexed by BOLD signal increases relative to the categorization baseline, while suppression was indexed by BOLD signal decreases relative to categorization baseline. These indices were extracted from DN and FPCN subnetworks, and from the visual network.

The DN subnetworks, FPCN-A, and the visual network showed distinct patterns of enhancement and suppression (Fig. 4 and *SI Appendix*, Table S7). Consistent with its role in executive control (23), including attention and inhibition, FPCN-A exhibited enhanced activation during both task-relevant and task-irrelevant trials relative to nonselective perceptual categorization. In contrast, the DN and visual networks demonstrated context-dependent neuromodulation. DN-A and DN-B showed enhanced activation during task-relevant trials but suppressed activation during task-irrelevant trials relative to nonselective perceptual categorization. Suppression relative to categorization within these DN subnetworks reached group-level significance only for anonymous trials. The lack of DN suppression relative to categorization during task-irrelevant trials involving famous stimuli might reflect the interference of prior knowledge associations with the effective deployment of inhibitory control, consistent with the behavioral performance observed in these trials. The Temp-Par and Limbic networks from the extended DN showed suppression during task-irrelevant trials relative to categorization, but no enhancement. Finally, the visual network displayed the opposite pattern to the DN, with enhanced activation during task-irrelevant trials and suppression during task-relevant trials relative to nonselective perceptual categorization.

Selective Attention Shifts Brain Activity Along the Principal Gradient. Our results suggest that, unlike perceptually guided selective attention, which recruits sensory regions, selective attention involving memory processes involves coactivation between FPCN regions and DN regions. This raises the question of whether selective attention is underpinned by the modulation of neural activity along the principal gradient which differentiates unimodal and heteromodal cortices (Fig. 3*D*). This principal gradient accounts for the largest variance in macroscale task-free FC, underscoring its role as a behaviorally relevant brain state (70) that separates sensory from higher-order cognitive processes, including those supported by both DN and FPCN regions (43). To test this possibility, we computed the spatial correlation between the unthresholded selective attention effect map (*SI Appendix*, Fig. S3*B*) and the principal gradient map computed by Margulies et al. (43) based on an independent task-free fMRI dataset (for a similar approach, see ref. 50). This revealed a statistically significant positive correlation between the position along the gradient and the strength of modulation by selective attention ($r = 0.432$, $P = 0.015$). Specifically, the more a voxel's task-free FC resembled the heteromodal end of the principal gradient the stronger its activation to goal-relevant versus irrelevant trials. These results suggest that selective attention involving memory processes dynamically shifts brain activity between sensory cortices and higher-order heteromodal regions, depending on task demands.

We then identified the specific portions of the principal gradient that showed a reliable task relevance effect. To this end, we divided voxels into ten bins based on their position along the gradient—lower bin values correspond to voxels closer to the unimodal end, while higher bin values correspond to voxels closer to the heteromodal end. Only Bins 9 and 10, representing the heteromodal extreme of the gradient (which includes DN and FPCN regions, see ref. 43), were reliably engaged by relevant compared to irrelevant stimuli, while Bin 8 approached significance (Fig. 3*D* and *SI Appendix*, Table S5). These findings suggest that selective working memory is supported by heteromodal regions located at the top-end of the principal gradient.

Reliable engagement of heteromodal cortices was also observed for attentional selection relative to the categorization control condition (*SI Appendix*, *Result* and Fig. S5). This analysis also showed that nonselective perceptual decisions reliably engaged Bin 2 located at the unimodal end of the principal gradient. This finding aligns with the view that decisions guided by memory and those based on available perceptual input recruit opposite ends of the principal gradient (40–42).

Discussion

The capacity to selectively attend to incoming information based on goal-relevance has been largely studied through the lens of perceptual features (e.g., size, shape, perceptual category) of stimuli lacking long-term memory associations. In everyday life, what we selectively attend to is also determined by our prior knowledge, and the targets of attention are often familiar. Yet, there have been relatively fewer studies examining selective attention guided by prior knowledge. The primary aim of the current study was to examine the neural correlates of selective attention, focusing on how memory-independent (anonymous) versus memory-enhanced (famous) stimuli are selected for working memory-based decision-making amid distractors. Our findings offer valuable insights into how the brain enables the interplay between selective attention and memory retrieval, highlighting a role for the DN in actively supporting selective working memory when task relevance is determined by long-term memory associations.

We first provided behavioral evidence that selective attention can be either enhanced or hindered by prior knowledge associations during a working memory task, depending on the goal relevance of that prior knowledge. Next, we demonstrated that DN brain regions were preferentially engaged by famous relative to anonymous stimuli, consistent with our previous findings that the DN serves as a gateway to stored prior knowledge representations in the service of goal-directed cognition (47). In contrast to previous investigations that implicate coactivation of control and sensory regions in perceptually guided selective attention, here we showed that selective attention involving memory processes depends on extensive coactivation across frontal, temporal, and parietal cortices belonging to the FPCN and DN. Specifically, we observed that task-relevant stimuli increased activation in the frontal poles, posterior middle temporal gyrus and anterior inferior parietal lobule of the FPCN-A subnetwork, the medial prefrontal

cortex and posterior cingulate cortex of DN-A, the inferior and superior frontal gyri, lateral temporal cortex, and angular gyri of DN-B, the superior temporal gyri of the Temp-Par subnetwork, and the ventromedial, orbitofrontal, and anteroventral temporal cortices of the Limbic subnetwork within the extended DN. We demonstrated that DN and visual cortex responses during selective attention were driven by opposing patterns of context-dependent enhancement and suppression relative to nonselective perceptual processing, which is characteristic of top–down neuromodulation. Critically, in line with a role for the DN in long-term memory, only the DN exhibited a fame-dependent task-relevance effect. Specifically, the DN exhibited suppressed activation for task-irrelevant trials relative to perceptual categorization only in response to memory-independent (anonymous), but not memory-enhanced (famous) stimuli. Finally, we demonstrated that selective working memory modulates brain activation along the unimodal-to-heteromodal principal gradient. Whole brain activation observed during the selection of goal-relevant stimuli was observed in higher-order heteromodal cortices, including DN regions, consistent with reliance on internally oriented and perceptually decoupled thought. Collectively, our findings reveal that selective attention is supported by a top–down modulatory mechanism involving coactivation of frontoparietal control and default regions, suggesting that attentional control can interact with either memory or perception in the service of goal directed cognition, and these are subserved by different neural mechanisms.

Default Network Involvement In Interactions Between Selective Attention and Memory. We replicated previous findings implicating the DN in retrieval of long-term memories (31, 36, 37, 71), including knowledge about unique entities (47, 72, 73), by showing that famous stimuli activated DN regions regardless of stimulus domain. Stored knowledge about unique entities, such as familiar people and landmarks, differs from other types of prior knowledge because it includes proper names and idiosyncratic semantic and autobiographical associations (72). These unique attributes put them at the extreme of a semantic specificity continuum spanning from unique (e.g., Empire State Building, Barak Obama) to less specific (building, president) to general categories (human-made objects, humans). The effect of fame on brain activity was accompanied by enhanced behavioral performance for famous relative to anonymous stimuli when fame was aligned with task goals. This behavioral effect may reflect the benefits of semantic elaboration on episodic encoding (74). Alternatively, the association of famous stimuli with proper names could support a rehearsal strategy aiding working memory maintenance, though this seems unlikely given the variable number of intervening stimuli between N-back matches and weak evidence for articulatory rehearsal benefits in working memory (75). In contrast, during task-irrelevant trials, fame was associated with reduced behavioral performance, suggesting greater attentional capture by famous stimuli. This heightened distraction may explain why the DN was suppressed only for anonymous but not famous task-irrelevant stimuli. The negative behavioral effect of fame on task-irrelevant trials was stronger for famous faces than places, consistent with our observation of greater DN responsiveness to famous faces. This may be attributed to the higher attentional salience of faces (76), and greater DN recruitment during social, as opposed to nonsocial, information processing (62, 63). These results demonstrate that prior knowledge can both benefit and hinder cognitive control depending on goal relevance.

In a data-driven multivariate analysis, we found that selective working memory modulated DN activity. Task-relevant trials elicited greater DN activation compared to irrelevant trials. Unlike irrelevant trials, relevant trials involved comparing percepts with information stored in working memory and encoding them for future goal-directed use. As prior research implicates the DN in the retrieval rather than the encoding stage of episodic memory (77–79), DN's specific contribution to task relevant stimuli likely reflects the prioritization of memory representations of previous trials. This interpretation is consistent with research implicating the DN in decisions based on working memory contents rather than on available perceptual inputs, even when the stimuli lack long-term memory associations (40, 41, 80, 81). Given its maximal physical and functional distance from sensorimotor areas (43), it has been suggested that DN is optimally suited to support *perceptually decoupled,* memory-guided cognition (43, 44). Thus, our findings support the proposed link between DN and perceptual-decoupling, and extend it by showing that DN recruitment during memory-guided thought and action is not purely automatic (cf., 82), but can also be subject to top–down attentional control. In other words, DN engagement might reflect a working memory signal that is gated by goal relevance via top–down control signals (cf., 1, 83, 84).

At the subnetwork level, selective attention reliably modulated most subnetworks within the extended DN, including medial and lateral frontoparietal cortices, as well as lateral temporal cortex, but not DN-C, which comprises the medial temporal, retrosplenial, and posteroventral parietal cortices. The lack of a reliable effect in DN-C may be due to differential responses in its anterior and posterior portions: Anterior medial temporal lobe regions, particularly in the left hemisphere, responded preferentially to task-relevant stimuli, while posterior regions responded more to irrelevant stimuli. This aligns with well-documented functional distinctions along the medial temporal lobe's anterior–posterior axis, which have been linked to several potential factors, including processing gist versus details, and entities versus context (85, 86). While the underlying drivers remain unclear, our findings reinforce the broader literature on anterior–posterior functional specialization within DN-C.

We expected that, given its role in long-term memory retrieval, DN activity would be more strongly modulated by selective attention to memory-enhanced (famous) compared to memory-independent (anonymous) stimuli. Such a pattern would mirror the response of sensory regions specialized for processing task-relevant perceptual features during perceptually guided selective attention (e.g., ref. 10). Contrary to this expectation, we found comparable DN responses to relevant trials regardless of stimulus fame in the whole-brain analyses. This could be due to the fact that, although unfamiliar faces and places lack unique long-term memory associations, they can trigger retrieval of memories of distinct yet similar unique entities or more generic prior knowledge (e.g., social categories and associated stereotypes) which also engages DN regions (87–89). Furthermore, determining whether a stimulus is anonymous or famous requires an active search of long-term memory, which could itself recruit the DN. As a result, interleaving famous and anonymous stimuli may reduce sensitivity to more subtle fame effects. Methodological approaches that can disentangle selective attention based on prior knowledge from the subsequent decision stage (cf., 90), along with more precise experimental manipulations of access to prior knowledge during cognitive control tasks, will be critical for clarifying the DN's role in the interplay between long-term memory access and selective attention. Nevertheless, the finding that famous stimuli elicited a different pattern of context-dependent enhancement and suppression relative to anonymous stimuli specifically in the DN suggests that DN modulation by selective attention is sensitive to the richer mnemonic content of familiar stimuli.

Altogether, these findings suggest that the DN fulfills distinct roles during selective working memory guided by prior knowledge. Its greater activation to famous versus anonymous faces and places highlights its importance for representing prior knowledge, and, by extension, assessing goal relevance to guide attentional selection. Its enhancement by task-relevant stimuli and suppression by irrelevant stimuli highlights its contribution to working memory, supporting the prioritization of working memory when goal relevant and its inhibition when encountering distractors. Finally, the fame-dependent effect of task relevance on DN suppression might suggest an interplay between automatic long-term memory retrieval and goal-relevance-gated working memory.

Implications for Neurocognitive Theories of Selective Attention. Contemporary theories of selective attention ascribe a key role of top–down modulation of sensory cortices by control signals from the FPCN and DAN (66, 91–93). These theories predict coactivation of both prefrontal control regions and sensory areas specialized for processing task-relevant information during attentional selection. In line with these models, we observed sustained coactivation of FPCN and DAN regions during the selective N-back working memory task compared to the nonselective Categorization task. However, contrary to these predictions, within the N-back task block, we observed opposing transient responses in prefrontal control and sensory regions: Compared to irrelevant trials, relevant trials increased FPCN activation but reduced visual network activation. Relative visual network disengagement during task-relevant trials likely reflects a temporary reallocation of cognitive resources away from detailed perceptual processing of the immediate sensory input to enable comparison between the current percept and representations of previous trials stored in higher-order cortices. Two additional findings support this interpretation. First, our control analysis showed that the visual network responded to both irrelevant N-back trials and categorization trials. This suggests that its activation was driven by lower-level processes and is consistent with its well-documented role in online visual processing (94, 95). Second, modulation of visual cortex activation by selective attention reflected suppression during relevant trials but enhancement during irrelevant trials relative to the perceptual categorization baseline. This demonstrates that, rather than being a general effect, suppression occurred specifically during trials that required decisions based on working memory contents. Our interpretation is consistent with single-unit studies in macaques showing that early visual areas primarily encode perceptual information, whereas downstream higher-order association regions contain neuronal populations that represent both percepts and working-memory contents (96). Recent fMRI work in humans further shows that spatial tuning in visual cortex is weaker, less precise, and less variable across visual areas during working memory maintenance compared to tuning during bottom–up visual processing (97). Such findings challenge the view that working memory critically depends on sensory reactivation (98). One explanation of prior reports of increased sensory cortex BOLD activity during selective attention and working memory is that such activity reflects top–down feedback from higher-order regions rather than bottom–up perceptual processes (99, 100). This view is consistent with evidence that, in some contexts, the BOLD signal tracks local field potentials more closely than neuronal spiking activity (101). Under this account, the observed enhancement of visual network activity for stimuli that had to be ignored could reflect increased inhibitory top–down input from cognitive control regions, whereas suppression for task-relevant stimuli might reflect release from such inhibitory input. Critically, this interpretation rests on the hypothesis that BOLD reflects incoming synaptic input more closely than local neuronal output, with top–down modulatory signals influencing the former more than the latter (99), and it remains to be directly tested. Our findings contribute to this body of evidence by suggesting that the momentary suppression of the BOLD response in the visual cortex is a crucial mechanism of selective working memory.

Past research reported preferential processing of goal-irrelevant information in the DN instead of sensory regions (102, 103). Contrary to this, we found that task-relevant, rather than irrelevant trials, elicited DN activation. This pattern was observed even though relevant trials were more difficult, as revealed by less accurate and slower behavioral responses, and demonstrates that the DN can contribute actively to cognitive control tasks, challenging the traditional "task-negative" view of DN function (104). Two results are consistent with this idea. First, DN activation was modulated by task-relevant versus irrelevant N-back trials, but not by Categorization trials, which did not impose cognitive demands on working memory or selective attention. This shows that DN activation was specific to trials that required greater top–down control. Second, the pattern of task-dependent enhancement and suppression of DN activity relative to baseline is consistent with the neural signature of top–down modulation. The combination of enhancement and suppression generates a neural contrast that shapes processing to suit changing task demands and is reliably observed in sensory regions during perceptually guided selective attention (10, 105). This suggests that, when attentional selection is based on the availability of long-term memory associations and involves decisions based on working memory contents, the DN exhibits a response pattern consistent with that observed in sensory regions during perceptually guided selective attention.

We also demonstrated that FPCN's contribution to selective attention extends to a context in which the goal relevance of stimuli depends on prior knowledge rather than external perceptual information. This finding is consistent with FPCN's role as a key source of top–down control (12–14). Challenging its purported antagonistic relationship with the DN (106), we observed coactivation of these two networks during selective working memory. Along with recent studies showing activation of both networks during cognitive control tasks requiring memory retrieval (47–50), as well as flexible encoding of goal-relevant information in the local activity patterns of both networks (107, 108), our findings demonstrate that FPCN and DN can coactivate to support selective attention. This underscores the cognitive relevance of the principal gradient that highlights similarities in the task-free FC of DN and FPCN (43), and thus, a propensity for FPCN-DN collaboration. The importance of FPCN-DN collaboration in goal-directed cognition is further supported by the fact that both networks contain regions that exhibit preferential coupling with the other network. The left inferior frontal gyrus and posterior middle temporal gyrus within DN-B, which are key for the controlled retrieval of long-term memory (109–111), show strong coupling with FPCN regions (112, 113). Conversely, the FPCN-A subnetwork shows preferential coupling with DN regions (52) and was the only FPCN subnetwork reliably activated by goal-relevant trials in the current study (also see ref. 30). Unlike the DN, which showed only transient activation to relevant trials and context-dependent enhancement and suppression, the FPCN displayed sustained activation throughout the N-back task blocks, and enhancement regardless of task-relevance. This suggests that DN and FPCN make distinct contributions to selective working memory. Specifically, the FPCN's response pattern is consistent with a broader role in top–down control, encompassing both the selection of attentional targets for further goal-directed processing and the inhibition of distractors. This interpretation

aligns with extensive evidence for the FPCN's domain-general involvement in executive functions (114–116).

Finally, we showed that selective attention modulates activation along the unimodal-to-heteromodal dimension of macroscale functional organization. This suggests a push–pull relationship between unimodal regions (e.g., the visual network), and heteromodal regions (i.e., the DN), depending on whether the current goal requires prioritizing perceptual or memory information. The FPCN is optimally suited to mediate this relationship, given its characteristic ability to flexibly adjust its coupling with other brain regions across tasks (25). For example, the FPCN increases its functional coupling with either the DAN or DN depending on whether the task demands externally oriented attention or internally generated (e.g., memory) representations (30, 49, 117, 118). In the context of selective attention, FPCN couples with sensory regions when perceptual features determine task relevance (24, 92) or, as shown here, coactivates with the DN when access to prior knowledge can support cognitive control. The context-dependent and flexible FPCN engagement aligns with its role in orchestrating the dynamic allocation of cognitive resources based on goals (23). The internal organization of the FPCN may enhance its ability to coordinate with regions at either end of the principal gradient. Specifically, the FPCN-A and FPCN-B subnetworks exhibit preferential functional coupling with perceptually decoupled (DN) vs coupled (DAN) processing streams (52). Spatially intermediate FPCN regions show an intermediary functional profile suggestive of integration of information arising from these relatively segregated neural pathways (119, see also 112, 120, 121).

Our findings contribute to a growing body of research on the neural bases of interactions between attention and memory systems (1, 2, 66, 122, 123). Studies of visuospatial orienting guided by episodic associations similarly implicate FPCN regions, but do not report DN engagement, suggesting partly distinct neural correlates for prior knowledge-guided spatial attention versus prior knowledge-guided selective working memory (124). In contrast, studies examining selection among items maintained in working memory implicate not only FPCN regions but also regions affiliated with the DN, including the angular gyrus and inferior frontal gyrus (29, 84, 125). Likewise, a study comparing selection among competing perceptual inputs with selection among working memory representations reported preferential engagement of the left inferior frontal gyrus, a DN node, in the latter condition (126). Although these effects were more spatially restricted than the widespread DN engagement observed here, they similarly point to a role for DN regions in selective attention operating over working memory representations. Critically, however, these prior studies focus on selection among representations already maintained in working memory, whereas our task manipulation targets the goal-directed selection and prioritization of perceived stimuli for subsequent working memory processing. Studies comparing external attention, in which attention is directed toward perceptually available stimuli, with internal attention, in which attention is directed toward internally oriented, perceptually decoupled states, also implicate the DN. Greater DN activation and stronger within-DN FC has been observed during episodic retrieval relative to visual search or perceptual categorization (127, 128). A study using intracranial EEG found increased high-frequency activity (associated with the BOLD response) and decreased low frequency activity within the DN during autobiographical memory retrieval relative to visual search (129). Also, DN shows increased theta band connectivity with FPCN-A during spontaneous thought relative to auditory target detection (30). Together, these findings suggest a role for the DN in maintaining internal attention. To the extent that working memory reflects an attentional bias toward an internal state (1, 130), our findings extend this literature by demonstrating that goal-dependent modulation of DN activity supports top–down control over the engagement and suppression of internal attention.

Conclusions. This study examined the neural basis of selective attention beyond contexts that emphasize perceptual information, revealing how the brain enables attentional selection guided by prior knowledge. Our findings show that, unlike attention driven by perceptual features, the FPCN and DN work together to track changing task demands and support goal-directed attention deployment in the context of selective working memory. This suggests that selective attention might operate through distinct neural pathways depending on whether the current goal requires prioritizing perceptual information or memory contents. Notably, the FPCN may act as a switch between these pathways, enabling us to navigate the constant mix of novel and familiar sensory signals we experience in daily life. Returning to our real-world vignette from the Introduction, when deciding whether to disclose the acquaintance's personal health information during your conversation with a friend, the findings here suggest that the FPCN may help disengage attention from the immediate conversation anchored in the external environment, and shift it internally toward long-term memory, where coactivation with the DN supports the retrieval of relevant prior knowledge. This shift allows for a fluid conversation flow to continue while ensuring no improper sharing of a confidence. Given the seamless transitions between perceptually coupled versus uncoupled selective attention that are critically necessary for adaptive everyday functioning, understanding how selective attention interacts with memory, and the underlying neural mechanisms, is crucial. Future research is necessary to explore the unique contributions of different memory systems, such as those underpinning semantic versus autobiographical knowledge, as well as different component processes, such as relevance evaluation versus stimulus representation, and working memory encoding versus working-memory-based decision-making. This will be instrumental in developing a more comprehensive and ecologically valid neurocognitive account of flexible, goal-directed behavior.

Materials and Methods

Participants. A total of 34 young adults (M_{age} = 21.34, SD_{age} = 2.59, 17 women, 17 men) participated in the study. Three participants were excluded from the analyses because they did not complete a post-scan fame manipulation check (n = 1), or failed to correctly recognize at least 40% of famous stimuli (n = 2). Therefore, the final sample consisted of 31 participants, with ages ranging from 18 to 29 y (M_{age} = 21.37; SD_{age} = 2.55, 15 women, 16 men). All participants were right-handed, had normal or corrected-to-normal visual acuity and no history of psychiatric, neurological, or other medical illness that could compromise cognitive functions. All participants provided written informed consent. The study was approved by the Institutional Review Board of Cornell University.

Tasks. Participants performed two tasks during the scanning session, as detailed below. Responses were made on a button box placed in the participant's right hand.

N-Back Task. The experimental task was an adapted version of a famous faces N-back working memory task (47) to transiently evoke DN activity during a sustained working memory challenge, and aligns with the selective working memory paradigm previously used to probe perceptually guided selective attention (131). Participants were presented with a series of images of famous and anonymous faces and scenes (see Fig. 1 for examples) and were required to decide whether each image matched the image presented between one and four trials earlier.

Within each block, participants viewed interleaved famous and anonymous images and were instructed to focus on matching either the famous or the anonymous stimuli. This manipulation made famous trials task-relevant in the "Match Famous" blocks and irrelevant in the "Match Anonymous" blocks, with the reverse applying

to anonymous trials (Fig. 1*B*). Participants pressed one button for previously seen task-relevant stimuli and another for novel relevant stimuli and irrelevant stimuli.

To assess the generalizability of results across different stimulus categories, participants completed these tasks on face and scene images. In each block, participants were presented with either face or scene images, but never both stimulus types within the same block. This resulted in four types of N-back blocks: "Match Famous (Faces)", "Match Anonymous (Faces)", "Match Famous (Places)", and "Match Anonymous (Places)".

Categorization Task. Participants completed a control task in which they categorized each stimulus as either a face or a place. This task engaged bottom–up perceptual processing, automatic long-term memory access in the case of famous stimuli (132), and decision-making. Unlike the experimental task, it did not require working memory or selective attention.

MRI Data Acquisition and Preprocessing. In brief, brain imaging data were acquired using a 3T MRI scanner and included a T1-weighted structural used for normalization, as well as multiecho functional scans. Functional data were preprocessed and denoised using multiecho independent component analysis (119), followed by normalization to an MNI template and spatial smoothing with a 6-mm FWHM Gaussian kernel.

fMRI Data Analysis. Task-evoked whole brain activation patterns were analyzed using PLS (57, 58, 133). PLS is a data-driven multivariate analysis that can identify patterns of maximal covariance between voxel-wise brain activity and task conditions. Because of its ability to identify voxels with covarying activity, PLS is particularly well-suited for studying large-scale brain networks, which was the aim of the current study. Other advantages include that it does not require explicit modeling of the hemodynamic response and, by considering all voxels simultaneously, it avoids the problem of multiple statistical comparisons.

See *SI Appendix, Methods* for more detailed descriptions of the stimuli, experimental procedure, behavioral data analysis, MRI data acquisition and preprocessing, and fMRI data analysis.

Data, Materials, and Software Availability. Anonymized fMRI data, analysis scripts; and unthresholded group-level activation maps have been deposited in OpenNeuro (https://doi.org/10.18112/openneuro.ds007102.v1.0.0) (134) Open Science Framework (https://doi.org/10.17605/OSF.IO/BT8ZF) (135), and NeuroVault (https://identifiers.org/neurovault.collection:17919) (136).

ACKNOWLEDGMENTS. This work was supported by grants from the Canadian Institutes for Health Research and the NIH (1S10RR025145) (to R.N.S.), NSERC (to R.N.S. and G.R.T), and a postdoctoral fellowship from Fonds de Recherche du Quebec (345314) (to V.D.).

Author affiliations: [a]Montreal Neurological Institute, Department of Neurology and Neurosurgery, McGill University, Montreal, QC H3A 2B4, Canada; [b]Department of Psychology, Harvard University, Cambridge, MA 02138; [c]Department of Psychology, York University, Toronto, ON M3J 1P3, Canada; [d]McConnell Brain Imaging Centre, McGill University, Montreal, QC H3A 2B4, Canada; [e]Department of Psychiatry, McGill University, Montreal, QC H3A 1A1, Canada; and [f]Department of Psychology, McGill University, Montreal, QC H3A 1G1, Canada

1. K. Oberauer, Working memory and attention–A conceptual analysis and review. *J. Cogn.* **2**, 36 (2019).
2. N. Cowan *et al.*, The relation between attention and memory. *Annu. Rev. Psychol.* **75**, 183–214 (2024).
3. R. Desimone, J. Duncan, Neural mechanisms of selective visual attention. *Annu. Rev. Neurosci* **18**, 193–222 (1995).
4. J. H. R. Maunsell, S. Treue, Feature-based attention in visual cortex. *Trends Neurosci.* **29**, 317–322 (2006).
5. S. Yantis, J. T. Serences, Cortical mechanisms of space-based and object-based attentional control. *Curr. Opin. Neurobiol.* **13**, 187–193 (2003).
6. A. Gazzaley, Influence of early attentional modulation on working memory. *Neuropsychologia* **49**, 1410–1424 (2011).
7. D. C. Somers, S. L. Sheremata, Attention maps in the brain. *Wiley Interdiscip. Rev. Cogn. Sci.* **4**, 327–340 (2013).
8. J. C. Martinez-Trujillo, S. Treue, Feature-based attention increases the selectivity of population responses in primate visual cortex. *Curr. Biol.* **14**, 744–751 (2004).
9. B. C. Motter, Neural correlates of attentive selection for color or luminance in extrastriate area V4. *J. Neurosci.* **14**, 2178–2189 (1994).
10. A. Gazzaley, J. W. Cooney, K. McEvoy, R. T. Knight, M. D'Esposito, Top-down enhancement and suppression of the magnitude and speed of neural activity. *J. Cogn. Neurosci.* **17**, 507–517 (2005).
11. A.J.-W. Chen *et al.*, Goal-directed attention alters the tuning of object-based representations in extrastriate cortex. *Front. Hum. Neurosci.* **6**, 00187 (2012).
12. T. P. Zanto, M. T. Rubens, A. Thangavel, A. Gazzaley, Causal role of the prefrontal cortex in top-down modulation of visual processing and working memory. *Nat. Neurosci.* **14**, 656–661 (2011).
13. T. G. Lee, M. D'Esposito, The dynamic nature of top-down signals originating from prefrontal cortex: A combined fMRI–TMS study. *J. Neurosci.* **32**, 15458–15466 (2012).
14. D. Baldauf, R. Desimone, Neural mechanisms of object-based attention. *Science* **344**, 424–427 (2014).
15. J. L. Vincent, I. Kahn, A. Z. Snyder, M. E. Raichle, R. L. Buckner, Evidence for a frontoparietal control system revealed by intrinsic functional connectivity. *J. Neurophysiol.* **100**, 3328–3342 (2008).
16. R. M. Braga, R. L. Buckner, Parallel interdigitated distributed networks within the individual estimated by intrinsic functional connectivity. *Neuron* **95**, 457–471.e5 (2017).
17. M. D. Fox, M. Corbetta, A. Z. Snyder, J. L. Vincent, M. E. Raichle, Spontaneous neuronal activity distinguishes human dorsal and ventral attention systems. *Proc. Natl. Acad. Sci.* **103**, 10046–10051 (2006).
18. Y. Morishima *et al.*, Task-specific signal transmission from prefrontal cortex in visual selective attention. *Nat. Neurosci.* **12**, 85–91 (2009).
19. K. Heinen, E. Feredoes, N. Weiskopf, C. C. Ruff, J. Driver, Direct evidence for attention-dependent influences of the frontal eye-fields on feature-responsive visual cortex. *Cerebral Cortex* **24**, 2815–2821 (2014).
20. T. R. Marshall, J. O'Shea, O. Jensen, T. O. Bergmann, Frontal eye fields control attentional modulation of alpha and gamma oscillations in contralateral occipitoparietal cortex. *J. Neurosci.* **35**, 1638–1647 (2015).
21. R. Ptak, The frontoparietal attention network of the human brain: Action, saliency, and a priority map of the environment. *Neuroscientist* **18**, 502–515 (2012).
22. B. M. Crittenden, D. J. Mitchell, J. Duncan, Task encoding across the multiple demand cortex is consistent with a frontoparietal and cingulo-opercular dual networks distinction. *J. Neurosci.* **36**, 6147–6155 (2016).
23. J. Duncan, The multiple-demand (MD) system of the primate brain: Mental programs for intelligent behaviour. *Trends Cogn. Sci.* **14**, 172–179 (2010).
24. A. Gazzaley *et al.*, Functional interactions between prefrontal and visual association cortex contribute to top-down modulation of visual processing. *Cerebral Cortex* **17**, i125–i135 (2007).
25. M. W. Cole *et al.*, Multi-task connectivity reveals flexible hubs for adaptive task control. *Nature Neurosci.* **16**, 1348–1355 (2013).
26. M. Fischer, M. Moscovitch, C. Alain, A systematic review and meta-analysis of memory-guided attention: Frontal and parietal activation suggests involvement of fronto-parietal networks. *WIREs Cogn. Sci.* **12**, e1546 (2021).
27. K. Isenburg, T. M. Morin, M. L. Rosen, D. C. Somers, C. E. Stern, Functional network reconfiguration supporting memory-guided attention. *Cereb. Cortex.* **33**, 7702–7713 (2023).
28. F. van Ede, A. C. Nobre, Turning attention inside out: How working memory serves behavior. *Ann. Rev. Psychol.* **74**, 137–165 (2023).
29. A. C. Nobre, D. Gresch, How the brain shifts between external and internal attention. *Neuron* **113**, 2382–2398 (2025).
30. J. W. Y. Kam *et al.*, Default network and frontoparietal control network theta connectivity supports internal attention. *Nat. Hum. Behav.* **3**, 1263–1270 (2019).
31. J. R. Binder, R. H. Desai, W. W. Graves, L. L. Conant, Where is the semantic system? A critical review and meta-analysis of 120 functional neuroimaging studies *Cerebral Cortex* **19**, 2767–2796 (2009).
32. R. G. Benoit, D. L. Schacter, Specifying the core network supporting episodic simulation and episodic memory by activation likelihood estimation. *Neuropsychologia* **75**, 450–457 (2015).
33. M. Irish, D. Vatansever, Rethinking the episodic-semantic distinction from a gradient perspective. *Curr. Opin. Behav. Sci.* **32**, 43–49 (2020).
34. B. C. Dickerson, H. Eichenbaum, The episodic memory system: neurocircuitry and disorders. *Neuropsychopharmacol* **35**, 86–104 (2010).
35. M. A. Lambon Ralph, E. Jefferies, K. Patterson, T. T. Rogers, The neural and computational bases of semantic cognition. *Nat. Rev. Neurosci.* **18**, 42–55 (2017).
36. E. Svoboda, M. C. McKinnon, B. Levine, The functional neuroanatomy of autobiographical memory: A meta-analysis. *Neuropsychologia* **44**, 2189–2208 (2006).
37. A. F. Tanguay *et al.*, The shared and unique neural correlates of personal semantic, general semantic, and episodic memory. *eLife* **12**, e83645 (2023).
38. J. R. Andrews-Hanna, J. Smallwood, R. N. Spreng, The default network and self-generated thought: Component processes, dynamic control, and clinical relevance. *Ann. N.Y. Acad. Sci.* **1316**, 29–52 (2014).
39. V. Menon, 20 years of the default mode network: A review and synthesis. *Neuron* **111**, 2469–2487 (2023).
40. M. Konishi, D. G. McLaren, H. Engen, J. Smallwood, Shaped by the past: The default mode network supports cognition that is independent of immediate perceptual input. *PLOS ONE* **10**, e0132209 (2015).
41. C. Murphy *et al.*, Distant from input: Evidence of regions within the default mode network supporting perceptually-decoupled and conceptually-guided cognition. *NeuroImage* **171**, 393–401 (2018).
42. C. Murphy *et al.*, Modes of operation: A topographic neural gradient supporting stimulus dependent and independent cognition. *NeuroImage* **186**, 487–496 (2019).
43. D. S. Margulies *et al.*, Situating the default-mode network along a principal gradient of macroscale cortical organization. *Proc. Natl. Acad. Sci.* **113**, 12574–12579 (2016).
44. J. Smallwood *et al.*, The default mode network in cognition: A topographical perspective. *Nat. Rev. Neurosci.* **22**, 503–513 (2021).
45. R. L. Buckner, L. M. DiNicola, The brain's default network: Updated anatomy, physiology and evolving insights. *Nat. Rev. Neurosci.* **20**, 593–608 (2019).
46. W. D. Stevens, R. N. Spreng, Resting-state functional connectivity MRI reveals active processes central to cognition. *WIREs Cogn. Sci.* **5**, 233–245 (2014).
47. R. N. Spreng *et al.*, Goal-congruent default network activity facilitates cognitive control. *J. Neurosci.* **34**, 14108–14114 (2014).
48. M. L. Meyer, R. P. Spunt, E. T. Berkman, S. E. Taylor, M. D. Lieberman, Evidence for social working memory from a parametric functional MRI study. *Proc. Natl. Acad. Sci.* **109**, 1883–1888 (2012).
49. R. N. Spreng, W. D. Stevens, J. P. Chamberlain, A. W. Gilmore, D. L. Schacter, Default network activity, coupled with the frontoparietal control network, supports goal-directed cognition. *NeuroImage* **53**, 303–317 (2010).
50. X. Wang *et al.*, Macroscale brain states support the control of semantic cognition. *Commun. Biol.* **7**, 1–17 (2024).
51. H. Kim, Default network activation during episodic and semantic memory retrieval: A selective meta-analytic comparison. *Neuropsychologia* **80**, 35–46 (2016).
52. M. L. Dixon *et al.*, Heterogeneity within the frontoparietal control network and its relationship to the default and dorsal attention networks. *Proc. Natl. Acad. Sci.* **115**, E1598–E1607 (2018).
53. B. T. Yeo *et al.*, The organization of the human cerebral cortex estimated by intrinsic functional connectivity. *J. Neurophysiol.* **106**, 1125–1165 (2011).

54. M. C. Jackson, J. E. Raymond, Familiarity enhances visual working memory for faces. *J. Exp. Psychol. Hum. Percept. Perform.* **34**, 556–568 (2008).
55. W. Xie, W. Zhang, Familiarity increases the number of remembered Pokémon in visual short-term memory. *Mem. Cogn.* **45**, 677–689 (2017).
56. W. P. Banks, Signal detection theory and human memory. *Psychol. Bull.* **74**, 81–99 (1970).
57. A. R. McIntosh, F. L. Bookstein, J. V. Haxby, C. L. Grady, Spatial pattern analysis of functional brain images using partial least squares. *Neuroimage* **3**, 143–157 (1996).
58. A. Krishnan, L. J. Williams, A. R. McIntosh, H. Abdi, Partial Least Squares (PLS) methods for neuroimaging: A tutorial and review. *NeuroImage* **56**, 455–475 (2011).
59. R. Kong *et al.*, A network correspondence toolbox for quantitative evaluation of novel neuroimaging results. bioXriv [Preprint] (2024), https://www.biorxiv.org/content/10.1101/2024.060.170.599426v1 [Accessed 10 July 2024].
60. N. Kanwisher, G. Yovel, The fusiform face area: A cortical region specialized for the perception of faces. *Philos. Trans. R. Soc. B: Biol. Sci.* **361**, 2109–2128 (2006).
61. R. Epstein, N. Kanwisher, A cortical representation of the local visual environment. *Nature* **392**, 598–601 (1998).
62. I. F. Tso, S. Rutherford, Y. Fang, M. Angstadt, S. F. Taylor, The "social brain" is highly sensitive to the mere presence of social information: An automated meta-analysis and an independent study. *PLOS ONE* **13**, e0196503 (2018).
63. D. I. Tamir, A. B. Bricker, D. Dodell-Feder, J. P. Mitchell, Reading fiction and reading minds: The role of simulation in the default network. *Soc. Cogn. Affect. Neurosci.* **11**, 215–224 (2016).
64. R. N. Spreng, C. L. Grady, Patterns of brain activity supporting autobiographical memory, prospection, and theory of mind, and their relationship to the default mode network. *J. Cogn. Neurosci.* **22**, 1112–1123 (2010).
65. D. R. Addis, A. R. McIntosh, M. Moscovitch, A. P. Crawley, M. P. McAndrews, Characterizing spatial and temporal features of autobiographical memory retrieval networks: A partial least squares approach. *NeuroImage* **23**, 1460–1471 (2004).
66. A. Gazzaley, A. C. Nobre, Top-down modulation: Bridging selective attention and working memory. *Trends Cogn. Sci.* **16**, 129–135 (2012).
67. M. Girn, R. Setton, G. R. Turner, R. N. Spreng, The "limbic network", comprising orbitofrontal and anterior temporal cortex, is part of an extended default network: Evidence from multi-echo fMRI. *Network Neurosci.* **8**, 860–882 (2024).
68. R. Kong *et al.*, Individual-specific areal-level parcellations improve functional connectivity prediction of behavior. *Cerebral Cortex* **31**, 4477–4500 (2021).
69. A. Gazzaley, J. W. Cooney, J. Rissman, M. D'Esposito, Top-down suppression deficit underlies working memory impairment in normal aging. *Nat. Neurosci.* **8**, 1298–1300 (2005).
70. A. S. Greene, C. Horien, D. Barson, D. Scheinost, R. T. Constable, Why is everyone talking about brain state? *Trends Neurosci.* **46**, 508–524 (2023).
71. L. Renoult, M. Irish, M. Moscovitch, M. D. Rugg, From knowing to remembering: The semantic-episodic distinction. *Trends Cogn. Sci.* **23**, 1041–1057 (2019).
72. L. A. Ross, I. R. Olson, What's Unique about Unique Entities? An fMRI Investigation of the Semantics of Famous Faces and Landmarks. *Cerebral Cortex* **22**, 2005–2015 (2012).
73. M. L. Gorno-Tempini, C. J. Price, Identification of famous faces and buildings: A functional neuroimaging study of semantically unique items. *Brain* **124**, 2087–2097 (2001).
74. F. I. M. Craik, E. Tulving, Depth of processing and the retention of words in episodic memory. *J. Exp. Psychol. Gen.* **104**, 268–294 (1975).
75. K. Oberauer, Is rehearsal an effective maintenance strategy for working memory? *Trends Cogn. Sci.* **23**, 798–809 (2019).
76. A. End, M. Gamer, Preferential processing of social features and their interplay with physical saliency in complex naturalistic scenes. *Front. Psychol.* **8**, 00418 (2017).
77. W. Huijbers, C. M. A. Pennartz, R. Cabeza, S. M. Daselaar, The hippocampus is coupled with the default network during memory retrieval but not during memory encoding. *PLOS ONE* **6**, e17463 (2011).
78. H. Kim, Encoding and retrieval along the long axis of the hippocampus and their relationships with dorsal attention and default mode networks: The HERNET model. *Hippocampus* **25**, 500–510 (2015).
79. S. M. Daselaar *et al.*, Posterior midline and ventral parietal activity is associated with retrieval success and encoding failure. *Front. Hum. Neurosci.* **3**, 13 (2009).
80. J. Smallwood *et al.*, Escaping the here and now: Evidence for a role of the default mode network in perceptually decoupled thought. *Neuroimage* **69**, 120–125 (2013).
81. C. Murphy *et al.*, Modes of operation: A topographic neural gradient supporting stimulus dependent and independent cognition. *NeuroImage* **186**, 487–496 (2019).
82. W. Schneider, R. M. Shiffrin, Controlled and automatic human information processing: I. Detection, search, and attention. *Psychol. Rev.* **84**, 1–66 (1977).
83. J. A. Elman, A. P. Shimamura, Task relevance modulates successful retrieval effects during explicit and implicit memory tests. *NeuroImage* **56**, 345–353 (2011).
84. G. Wallis, M. Stokes, H. Cousijn, M. Woolrich, A. C. Nobre, Frontoparietal and cingulo-opercular networks play dissociable roles in control of working memory. *J. Cogn. Neurosci.* **27**, 2019–2034 (2015).
85. J. Poppenk, H. R. Evensmoen, M. Moscovitch, L. Nadel, Long-axis specialization of the human hippocampus. *Trends Cogn. Sci.* **17**, 230–240 (2013).
86. C. Ranganath, M. Ritchey, Two cortical systems for memory-guided behaviour. *Nat. Rev. Neurosci.* **13**, 713–726 (2012).
87. A. Ishai, C. F. Schmidt, P. Boesiger, Face perception is mediated by a distributed cortical network. *Brain Res. Bull.* **67**, 87–93 (2005).
88. J. B. Freeman, K. L. Johnson, More than meets the eye: Split-second social perception. *Trends Cogn. Sci.* **20**, 362–374 (2016).
89. B. Deen, W. A. Freiwald, Parallel systems for social and spatial cognition reaching the cortical apex. *Proc. Natl. Acad. Sci.* **122**, e2520067122 (2025).
90. D. Moerel, A. N. Rich, A. Woolgar, Selective attention and decision-making have separable neural bases in space and time. *J. Neurosci.* **44**, e0224242024 (2024).
91. M. Corbetta, G. L. Shulman, Control of goal-directed and stimulus-driven attention in the brain. *Nat. Rev. Neurosci.* **3**, 201–215 (2002).
92. S. Kastner, L. G. Ungerleider, Mechanisms of visual attention in the human cortex. *Ann. Rev. Neurosci.* **23**, 315–341 (2000).
93. N. Kanwisher, E. Wojciulik, Visual attention: Insights from brain imaging. *Nat. Rev. Neurosci.* **1**, 91–100 (2000).
94. F. Tong, Primary visual cortex and visual awareness. *Nat. Rev. Neurosci.* **4**, 219–229 (2003).
95. K. Grill-Spector, R. Malach, The human visual cortex. *Ann. Rev. Neurosci.* **27**, 649–677 (2004).
96. M. Roussy, D. Mendoza-Halliday, J. C. Martinez-Trujillo, Neural substrates of visual perception and working memory: Two sides of the same coin or two different coins? *Front. Neural Circuits* **15**, 764177 (2021).
97. S. E. Favila, B. A. Kuhl, J. Winawer, Perception and memory have distinct spatial tuning properties in human visual cortex. *Nat. Commun.* **13**, 5864 (2022).
98. Y. Xu, Revisit once more the sensory storage account of visual working memory. *Visual Cognition* **28**, 433–446 (2020).
99. G. M. Boynton, Spikes, BOLD, attention, and awareness: A comparison of electrophysiological and fMRI signals in V1. *J. Vis.* **11**, 12 (2011).
100. T. van Kerkoerle, M. W. Self, P. R. Roelfsema, Layer-specificity in the effects of attention and working memory on activity in primary visual cortex. *Nat. Commun.* **8**, 13804 (2017).
101. A. Ekstrom, How and when the fMRI BOLD signal relates to underlying neural activity: The danger in dissociation. *Brain Res. Rev.* **62**, 233–244 (2010).
102. J. Z. Chadick, A. Gazzaley, Differential coupling of visual cortex with default or frontal-parietal network based on goals. *Nat. Neurosci.* **14**, 830–832 (2011).
103. B. A. Anderson, C. L. Folk, S. M. Courtney, Neural mechanisms of goal-contingent task disengagement: Response-irrelevant stimuli activate the default mode network. *Cortex* **81**, 221–230 (2016).
104. R. N. Spreng, The fallacy of a "task-negative" network. *Front. Psychol.* **3**, 145 (2012).
105. J. H. Reynolds, L. Chelazzi, Attentional modulation of visual processing. *Ann. Rev. Neurosci.* **27**, 611–647 (2004).
106. M. D. Fox *et al.*, The human brain is intrinsically organized into dynamic, anticorrelated functional networks. *Proc. Natl. Acad. Sci.* **102**, 9673–9678 (2005).
107. P. Kuhnke, M. Kiefer, G. Hartwigsen, Conceptual representations in the default, control and attention networks are task-dependent and cross-modal. *Brain Lang.* **244**, 105313 (2023).
108. X. Wang, Z. Gao, J. Smallwood, E. Jefferies, Both default and multiple-demand regions represent semantic goal information. *J. Neurosci.* **41**, 3679–3691 (2021).
109. R. L. Jackson, The neural correlates of semantic control revisited. *NeuroImage* **224**, 117444 (2021).
110. D. Vatansever, J. Smallwood, E. Jefferies, Varying demands for cognitive control reveals shared neural processes supporting semantic and episodic memory retrieval. *Nat. Commun.* **12**, 2134 (2021).
111. V. Diveica, K. Koldewyn, R. J. Binney, Establishing a role of the semantic control network in social cognitive processing: A meta-analysis of functional neuroimaging studies. *NeuroImage* **245**, 118702 (2021).
112. V. Diveica *et al.*, Graded functional organization in the left inferior frontal gyrus: Evidence from task-free and task-based functional connectivity. *Cerebral Cortex* **33**, bhad373 (2023), 10.1093/cercor/bhad373.
113. J. Davey *et al.*, Exploring the role of the posterior middle temporal gyrus in semantic cognition: Integration of anterior temporal lobe with executive processes. *Neuroimage* **137**, 165–177 (2016).
114. M. Assem, M. F. Glasser, D. C. Van Essen, J. Duncan, A domain-general cognitive core defined in multimodally parcellated human cortex. *Cereb Cortex* **30**, 4361–4380 (2020).
115. T. A. Niendam *et al.*, Meta-analytic evidence for a superordinate cognitive control network subserving diverse executive functions. *Cogn. Affect Behav. Neurosci.* **12**, 241–268 (2012).
116. E. Fedorenko, J. Duncan, N. Kanwisher, Broad domain generality in focal regions of frontal and parietal cortex. *Proc. Natl. Acad. Sci. U.S.A.* **110**, 16616–16621 (2013).
117. R. N. Spreng, J. Sepulcre, G. R. Turner, W. D. Stevens, D. L. Schacter, Intrinsic architecture underlying the relations among the default, dorsal attention, and frontoparietal control networks of the human brain. *J. Cogn. Neurosci.* **25**, 74–86 (2013).
118. W. Gao, W. Lin, Frontal parietal control network regulates the anti-correlated default and dorsal attention networks. *Human Brain Mapping* **33**, 192–202 (2012).
119. D. E. Nee, Integrative frontal-parietal dynamics supporting cognitive control. *eLife* **10**, e57244 (2021).
120. R. Chiou, E. Jefferies, J. Duncan, G. F. Humphreys, M. A. Lambon Ralph, A middle ground where executive control meets semantics: The neural substrates of semantic control are topographically sandwiched between the multiple-demand and default-mode systems. *Cerebral Cortex* **33**, 4512–4526 (2023).
121. R. Chiou, J. Duncan, E. Jefferies, M. A. L. Ralph, The dimensionality of neural coding for cognitive control is gradually transformed within the lateral prefrontal cortex. *J. Neurosci.* **45**, e0233242024 (2024).
122. J. B. Hutchinson, N. B. Turk-Browne, Memory-guided attention: Control from multiple memory systems. *Trends Cogn. Sci.* **16**, 576–579 (2012).
123. F. van Ede, A. C. Nobre, Turning attention inside out: How working memory serves behavior. *Annu. Rev. Psychol.* **74**, 137–165 (2023).
124. M. Fischer, M. Moscovitch, C. Alain, A systematic review and meta-analysis of memory-guided attention: Frontal and parietal activation suggests involvement of fronto-parietal networks. *WIREs Cogn. Sci.* **12**, e1546 (2021).
125. J. Lepsien, I. Thornton, A. C. Nobre, Modulation of working-memory maintenance by directed attention. *Neuropsychologia* **49**, 1569–1577 (2011).
126. D. E. Nee, J. Jonides, Common and distinct neural correlates of perceptual and memorial selection. *Neuroimage* **45**, 963–975 (2009).
127. Y. P. Li, Y. Wang, N. B. Turk-Browne, B. A. Kuhl, J. B. Hutchinson, Perception and memory retrieval states are reflected in distributed patterns of background functional connectivity. *NeuroImage* **276**, 120221 (2023).
128. C. Sestieri, G. L. Shulman, M. Corbetta, Attention to memory and the environment: Functional specialization and dynamic competition in human posterior parietal cortex. *J. Neurosci.* **30**, 8445–8456 (2010).
129. J. Hammer *et al.*, Antagonistic behavior of brain networks mediated by low-frequency oscillations: Electrophysiological dynamics during internal–external attention switching. *Commun. Biol.* **7**, 1105 (2024).
130. M. M. Chun, J. D. Golomb, N. B. Turk-Browne, A taxonomy of external and internal attention. *Ann. Rev. Psychol.* **62**, 73–101 (2011).
131. A.J.-W. Chen *et al.*, Training of goal-directed attention regulation enhances control over neural processing for individuals with brain injury. *Brain* **134**, 1541–1554 (2011).
132. M. I. Gobbini, J. V. Haxby, Neural systems for recognition of familiar faces. *Neuropsychologia* **45**, 32–41 (2007).
133. A. R. McIntosh, B. Mišić, Multivariate statistical analyses for neuroimaging data. *Annu. Rev. Psychol.* **64**, 499–525 (2013).
134. V. Diveica, R. Setton, G. R. Turner, R. N. Spreng, Famous faces and places project (FFP). OpenNeuro. https://doi.org/10.18112/openneuro.ds007102.v1.0.0. Deposited 11 February 2026.
135. V. Diveica, R. Setton, G. R. Turner, R. N. Spreng, Goal-directed modulation of the default network supports interactions between selective attention, working memory, and prior knowledge. Open Science Framework. https://doi.org/10.17605/OSF.IO/BT8ZF. Deposited 21 April 2025.
136. V. Diveica, R. Setton, G. R. Turner, R. N. Spreng, Goal-directed modulation of the default network supports interactions between selective attention, working memory, and prior knowledge. NeuroVault. https://identifiers.org/neurovault.collection:17919. Deposited 27 August 2024.

PNAS

Supporting Information for

Goal-directed modulation of the default network supports interactions between selective attention, working memory, and prior knowledge

Veronica Diveica*, Roni Setton, Gary R. Turner, R. Nathan Spreng*

*Veronica Diveica or Nathan Spreng.
Email: veronica.diveica@mcgill.ca or nathan.spreng@mcgill.ca

This PDF file includes:

Supplementary Methods.
Supplementary Results.
Figures S1 to S6.
Tables S1 to S8.
SI References.

Supplementary Methods

Stimuli. The stimuli included pictures of faces and scenes, which were further categorized by fame status - famous or anonymous (see Figure 1 for examples). Famous faces depicted widely recognized celebrities, while famous scenes showed well-known landmarks. Anonymous faces featured less-recognized international celebrities matched for attractiveness, and anonymous scenes depicted lesser-known landmarks matched for perceptual features. The stimulus set was normed in a separate cohort of young and old adults from Toronto, Canada. In total, there were 160 unique stimuli. Each stimulus was presented a maximum of three times during the scans.

Procedure. Participants completed five fMRI runs, each beginning and ending with 15 seconds of fixation. Within each run, there were five task blocks (four N-back blocks and one Categorization control block) separated by 30 seconds fixation periods. The order of task blocks was counterbalanced across runs and participants.

Each block began with a 3-second instruction screen indicating the task (i.e., match famous, match anonymous, or categorize all) and ended with a 3-second feedback screen showing the participant's accuracy for that block. Each block contained 47 trials. On each trial, a single stimulus appeared for 0.5 seconds, followed by a jittered fixation interval of 1, 1.5, 2, or 4 seconds drawn from an exponential distribution. This resulted in 93-second blocks.

Across runs, participants encountered 235 trials per condition, totaling 1175 trials. This included 140 task-relevant N-back repeat trials. To ensure task engagement, memory load varied from 1-back to 4-back, with the number of N-back repeat trials per load fixed as follows: 4 1-back, 28 2-back, 96 3-back, and 12 4-back. An additional 39 task-irrelevant N-back repeat trials served as distractors.

Transition frequencies between task-relevance conditions were matched at multiple levels: within runs (across selective attention task blocks), within participants (across runs), and across participants, ensuring that all N-back task blocks, runs, and participants experienced the same transition frequencies. This was achieved using five pseudo-randomized sequences matched on transition frequencies. In each sequence, the order of task-relevance conditions was fixed, but the specific stimulus for each condition was randomly selected from the available stimulus pool. Each participant completed all five sequences four times across the scanning session, with the order randomized.

Following the scanning session, participants completed a manipulation check in which they rated the fame of all faces and scene images on a 7-point Likert scale from 1 (not famous) to 7 (famous). These data were used to implement exclusion criteria at the trial and participant levels. To ensure that the fame manipulation was successful, famous stimuli that received a rating lower than four were excluded from the trial-level fMRI analyses. To ensure that participants had enough trials in each experimental condition, participants who correctly recognized less than 40% of famous face and scene stimuli were excluded from the analyses (n = 2).

Behavioral Data Analysis. Four metrics were used to assess behavioral performance: accuracy, RT (i.e., latency from stimulus onset to behavioral response), D prime (i.e., the ability to discriminate between "old" and "new" stimuli, calculated as the difference between the z-score of the hit rate and the z-score of the false alarm rate (1) and Criterion C (i.e., response bias, calculated as the negative average of the z-scores of the hit rate and the false alarm rate; a criterion of zero indicates no bias, a positive criterion indicates a conservative bias - preferring to say "new" - and a negative criterion indicates a liberal bias - preferring to say "old" (1).

Mixed effects models, as implemented in the R package "lme4" (2), were fitted on the behavioral data. The factors fame (famous vs. anonymous), domain (face vs. scene), task relevance (relevant vs irrelevant), and their interactions were included as fixed effects. Participant and stimulus ID were included as random intercepts to account for any systematic differences in performance between participants (e.g., processing speed) and specific face/scene stimuli. Linear mixed-effects models were fitted on RT, D prime, and Criterion C, whereas logistic mixed-effects models were fitted on accuracy data. Only trials including stimuli that were correctly rated as famous (at least 4 on the 7 point-Likert scale) in a post-scan manipulation check were analyzed to ensure that the participants had prior knowledge of the famous faces/places. RT analyses were performed on correct trials only. The R package "lmerTest" (3) was used to compute p-values for the estimated models via the Satterthwaite's degrees of freedom method. To explore interaction effects, simple slope analyses were conducted using the R package "emmeans" (4).

MRI Data Acquisition and Preprocessing. Brain imaging data were acquired with a 3T GE Discovery MR750 MRI scanner with a 32-channel receive-only phased-array head coil at the Cornell Magnetic Resonance Imaging Facility in Ithaca, New York. Anatomical scans were acquired using a T1-weighted volumetric MRI magnetization prepared rapid gradient echo (repetition time (TR) = 7 ms; echo time (TE) = 3.42 ms; 7° flip angle; 1.0 mm isotropic voxels, 176 slices). Five 10:03 min experimental runs of blood oxygen level-dependent (BOLD) functional scans were acquired with a T2*weighted multi-echo echo-planar imaging pulse sequence

(TR = 3000 ms; TE1=12.7ms; TE2= 27.39ms; TE3=42.50ms; 83° flip angle; field of view = 216 mm; 46 oblique slices; 3.0 mm isotropic voxels).

Anatomical images were skull-stripped using the default parameters in FSL BET (5). Functional images were preprocessed using multi-echo independent components analysis (ME-ICA; version 3.2 beta; https://github.com/ME-ICA/me-ica) (6), which builds on AFNI functions. ME-ICA relies on the TE-dependence model of the BOLD signal to determine T2∗ in every voxel and separates the BOLD signal from non-BOLD sources of noise. Before TE-dependent denoising, time series data were minimally preprocessed: the first 4 volumes were discarded and images were de-obliqued, slice-time corrected, and rigid body motion corrected. Volumes were then optimally combined across TEs and denoised. The optimally-combined and denoised (MEDN) voxel-wise time series outputs were registered from source space to MNI space using standard AFNI linear registration, resampled to 2.5-mm isotropic voxels in FSL (version 6.0.6.5), and spatially smoothed with a 6-mm FWHM Gaussian kernel using FSL SUSAN (7).

Partial Least Squares Analysis of fMRI Data. Task-evoked activation patterns were analyzed using partial least squares (PLS) (8–10) as implemented in the PLSgui/PLScmd toolbox for Matlab (https://www.rotman-baycrest.on.ca/index.php?section=84).

PLS does not require explicit modeling of the hemodynamic response. Instead, the BOLD signal for each voxel, for each person and task condition, is mean-centered, normalized to the block/event onset, and submitted to singular value decomposition. This process yields orthogonal latent variables (LVs), each representing distinct relationships between the brain data and the task conditions. Within each LV, each brain voxel is assigned a singular value weight or 'salience,' which is proportional to the covariance between its activity and the task conditions. Multiplying each salience value by the corresponding BOLD signal value for each voxel and then summing the product across all voxels gives a composite 'brain score' for each participant on each LV. This score reflects the extent to which a participant expresses the group pattern for that LV.

The statistical significance of each LV was determined via permutation testing involving 400 iterations of resampling without replacement. LVs were considered significant at $p < 0.05$. All reported LVs remain significant when using 1000 iterations. The reliability of each voxel's contribution to each LV was determined by calculating the standard error of each voxel's salience value across 100 bootstrapping iterations (resampling with replacement). Voxels' contributions were considered reliable if their absolute bootstrap ratios (BSR), calculated as the ratio of each voxel's salience to its standard error, exceeded 1.96, which is equivalent to $p < 0.05$. We confirmed that the whole-brain BSR pattern characterizing the main selective attention effect remains consistent when using 1000 bootstrapping iterations ($r = 0.998$, $p = 0.001$). The decomposition and associated resampling techniques consider all voxels simultaneously, thus avoiding the problem of multiple statistical comparisons.

The effects of task (N-back vs Categorization) and stimulus domain (Face N-back vs Place N-back) on neural activity were examined as blocks for the full block duration of 29 sec. The effect of fame as a function of stimulus domain (Famous Face vs Famous Place vs Anonymous Face vs Anonymous Place) and the effect of task relevance as a function of stimulus fame (Relevant Famous (Face/Place) vs Relevant Anonymous (Face/Place) vs Irrelevant Famous (Face/Place) vs Irrelevant Anonymous (Face/Place)), were examined as events spanning four TRs (i.e., first 9 sec post-stimulus onset) to encompass the typical time-window of the BOLD response peak. We confirmed that the main selective attention effect was reliable across windows up to 8 TRs (the first 21s after stimulus onset); we report the 4 TR results because the activation returned to baseline by that point. For these event-related analyses, only trials including stimuli that were correctly rated as famous (at least 4 on the 7 point-Likert scale) in a post-scan manipulation check were retained to ensure that the participants had prior knowledge of the famous faces/places. Moreover, to control for any recent memory effects, we analyzed only the first occurrence of each specific stimulus during the experimental conditions of interest. Only correct trials were included in the analyses of task relevance to avoid confounds arising from lapses in attention, misunderstanding of instructions, or other cognitive states unrelated to task demands. Because these data cleaning procedures resulted in variability in the number of trials retained for each analysis, we report the average number of trials per condition across participants in Table S8.

The results reported focus on the TR that showed the largest difference in brain scores between conditions: 9 sec post-stimulus onset for the fame by domain analysis (Lag1: $F(3, 90) = 17.56$, $p < .001$, $p\text{-eta}^2 = 0.37$; Lag2: $F(1.78, 53.52) = 23.01$, $p < .001$, $p\text{-eta}^2 = 0.43$; Lag3: $F(2.29, 68.72) = 26.28$, $p < .001$, $p\text{-eta}^2 = 0.47$), and 6 sec post-stimulus onset for the task relevance analyses (Lag1: $F(1.29, 38.79) = 90.72$, $p < .001$, $p\text{-eta}^2 = 0.75$; Lag2: $F(1.45, 43.44) = 143.29$, $p < .001$, $p\text{-eta}^2 = 0.83$; Lag3: $F(3, 90) = 43.15$, $p < .001$, $p\text{-eta}^2 = 0.59$). The temporal brain scores for all analyzed lags are displayed in Figure S6, whereas the activation maps for the other lags can be accessed via NeuroVault (https://identifiers.org/neurovault.collection:17919) and the Open Science Framework (https://doi.org/10.17605/OSF.IO/BT8ZF).

Estimation of Overlap Between Neural Patterns and Large-scale Functional Networks. Following the recommendations of Uddin et al. (11), we compared the result maps with an established cortical parcellation. We used the 7-network parcellation proposed by Yeo et al. (12). We measured overlap by computing the dice

coefficient (13) between the positive and negative LV expressions of our result maps (thresholded at |BSR| > 1.96) and each of the seven networks. We assessed the statistical significance of the dice coefficient using 1000 spin permutations as implemented in the "Neuromaps" Python package (14), a technique that accounts for spatial autocorrelation (15). Analyses were conducted in fsaverage surface space, with maps transformed from volume to surface space using Neuromaps' nonlinear transformation algorithm (16).

Statistical Comparison of Whole-Brain Map Similarity. Whole-brain map similarity was estimated by computing the product-moment correlation between voxels' values in the two maps. The statistical significance of the correlation coefficient was assessed using 1000 spin permutations, as described above. This procedure was used to compare the unthresholded whole-brain activity pattern distinguishing between relevant and irrelevant trials regardless of fame (Figure 3A) to the unthresholded maps resulting from the two control analyses (Figure S1), as well as with the principal FC gradient from Margulies et al. (17) (Figure 3D). This procedure was also used to compare the robustness of the activation map associated with the main effect of selective attention across different numbers of bootstrap iterations used to estimate the reliability of each voxel's contribution to the LV pattern.

Assessment of Reliability of Neural Effects at the Level of Gradient Bins and Sub-networks. To assess the reliability of the effect of selective attention at the gradient bin and sub-network levels, we extracted the mean BSR from the unthresholded result map masked with each bin/sub-network. The gradient bins were created by dividing the gradient values from Margulies et al. (17) into eleven equal intervals, resulting in ten bins. The DN sub-networks were defined using the 17-network parcellation from Yeo et al. (12) Additionally, the Limbic network from the 7-network parcellation, which includes the orbitofrontal and ventral anterior temporal lobes, was included due to recent evidence of its strong affiliation with the DN (18). Activation of an entire bin or sub-network was considered reliable only if the mean BSR value for all voxels within that bin or network was significantly above 1.96 (equivalent to $p < .05$), as determined by one-sample t-tests conducted using the "rstatix" R package (19). This procedure was also employed to assess the reliability of neural effects in visual regions from the probabilistic map by Wang et al. (20).

Evaluation of Network-level Enhancement and Suppression of Activation Magnitude Relative to the Categorization Baseline. We performed a GLM-based ROI analysis to estimate BOLD signal changes during selective working memory trials relative to the categorization trials in each (sub-)network of interest from Yeo et al. (12). The GLM was implemented using the "Nilearn" Python package (21), with one regressor per trial type modeled as a duration boxcar function convolved with the canonical Glover hemodynamic repsonse function. First-level whole-brain contrast maps were computed, and mean standardized t statistics were extracted from each network ROI by averaging voxel-wise values. Significant changes from baseline across participants were assessed using one-sample t-tests.

Supplementary Results

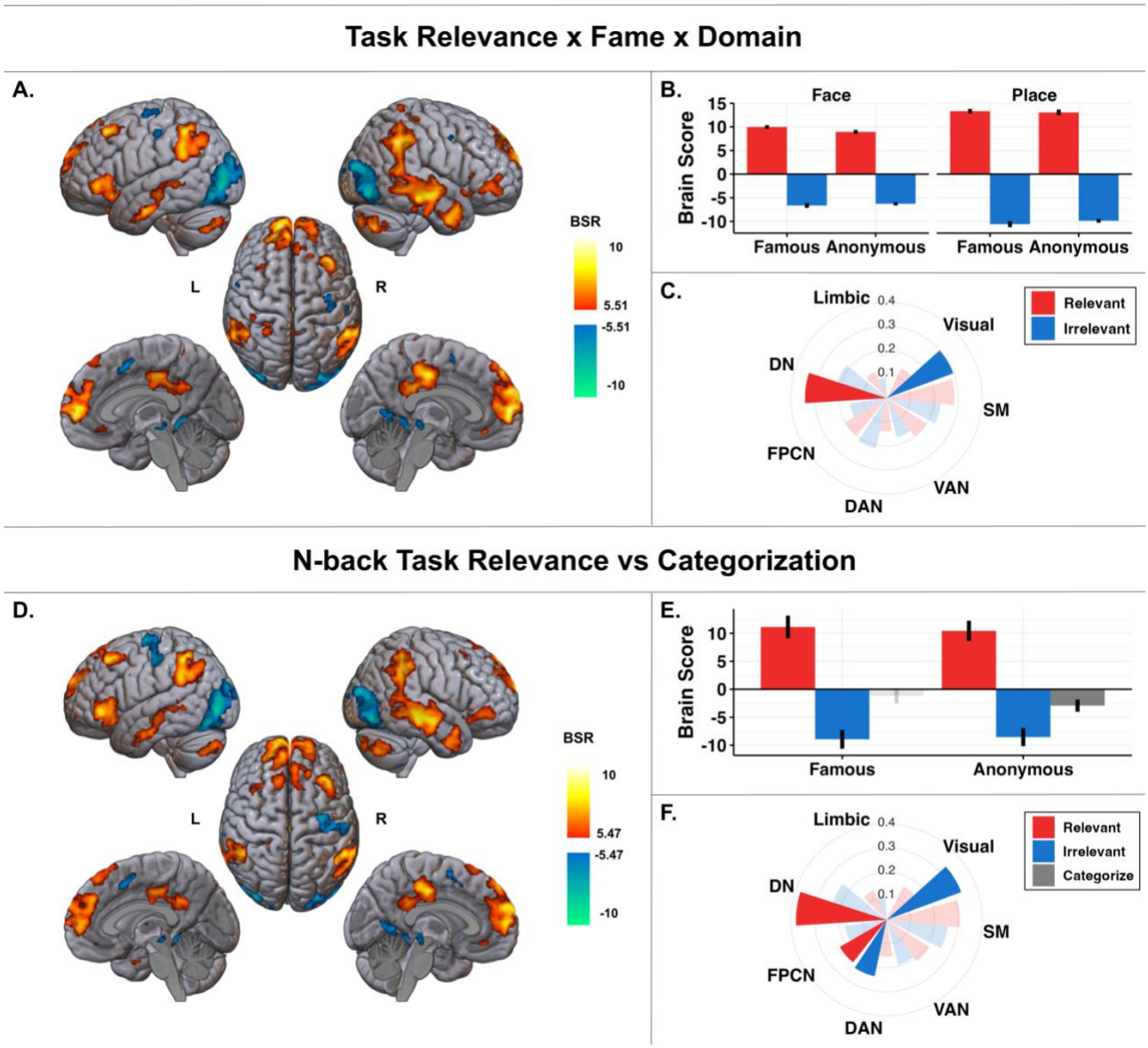

Fig. S1. Panels A-C. Differences in transient activity in response to relevant versus irrelevant trials irrespective of fame and domain. The maps show the top 5% of voxels based on BSR values (BSR > ± 5.51, equivalent to p < 3.58e-08). Panels D-F. Differences in transient activity during Relevant Famous/Anonymous trials relative to Irrelevant Famous/Anonymous and Categorized Anonymous trials. The maps show the top 5% of voxels based on BSR values (BSR > ± 5.47, p < 4.58e-08). Panels B/E. The mean brain scores (± SD) associated with the statistically significant LVs. Panels C/F. The degree of overlap between the brain patterns associated with the positive (red) and negative (blue) expression of the LV (thresholded at |BSR| > 1.96, p < .05) and the 7-network parcellation from Yeo et al. (12). Solid colors indicate statistically significant overlap, while transparent colors indicate non-significant overlap.

Patterns of Brain Activity are Modulated by the Visual Tasks Relative to Fixation. We conducted a PLS analysis to examine activation differences among N-back, Categorization, and Fixation (rest) blocks. A significant pattern of brain activity differentiated both task conditions from Fixation ($p < .001$), accounting for 92.28% of the covariance (Figure S2-B). Sustained N-back and Categorization performance was associated with increased BOLD activity in frontal control regions and posterior perceptual regions (Figure S2-A). This effect was evident across voxels in both lower-level and higher-order visual areas, with the strongest significance observed in ventral V2, ventral V3, and several higher-order temporal and parietal regions (Figure S3-A). In contrast, Fixation blocks were associated with activation in regions showing significant overlap with the DN and somatomotor networks (Figure S2-C), consistent with brain activation patterns observed during mind-wandering (22).

To better understand the topography of effects in visual cortex, we assessed the reliability of the neural pattern across voxels within cortical regions that contain topographic maps of visual space, as defined by Wang et al. (20). This analysis showed that sustained activation for visual tasks relative to fixation was observed across visual regions, reaching ROI-level significance in both low-level and higher-order visual cortices (Figure S3-A).

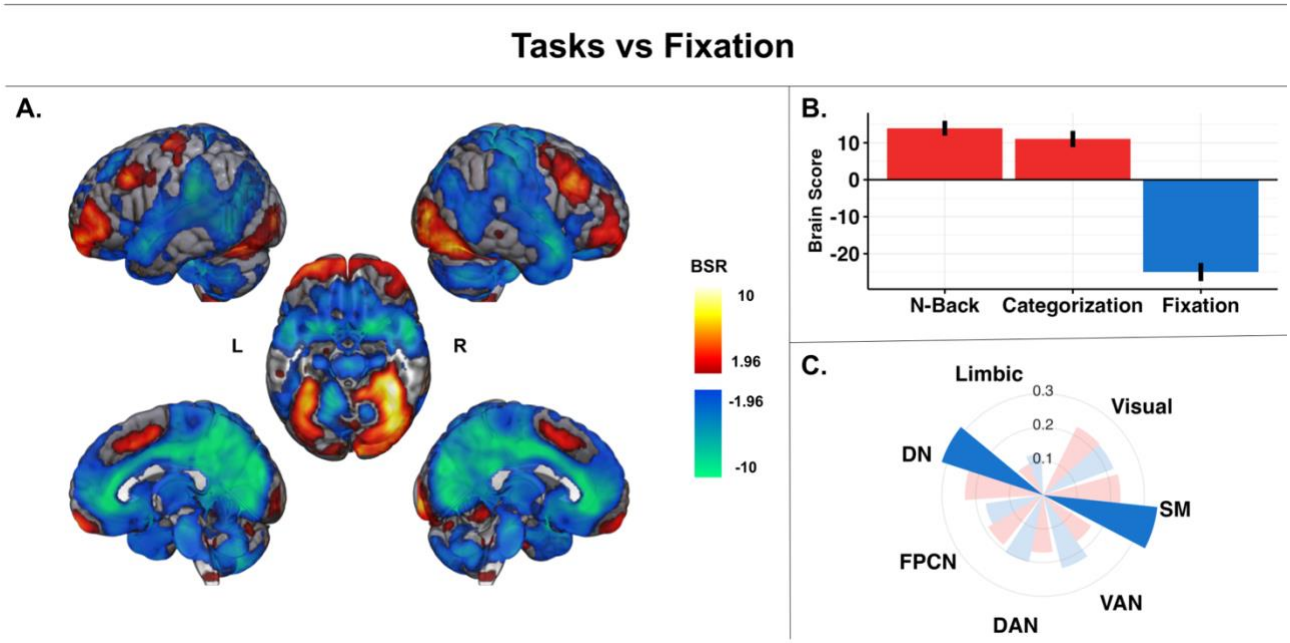

Fig S2. Differences in sustained activity in response to N-Back and Categorization tasks compared to the fixation rest blocks. Panel A. The maps show the voxels with BSR values ± 1.96 (equivalent to $p < 0.05$). Panel B. The mean brain scores (±SD) associated with the statistically significant LV. Panel C. The degree of overlap between the brain patterns associated with the positive (red) and negative (blue) expression of the LV (thresholded at $|BSR| > 1.96$, $p < .05$) and the 7-network parcellation from Yeo et al. (12). Solid colors indicate statistically significant overlap, while transparent colors indicate non-significant overlap.

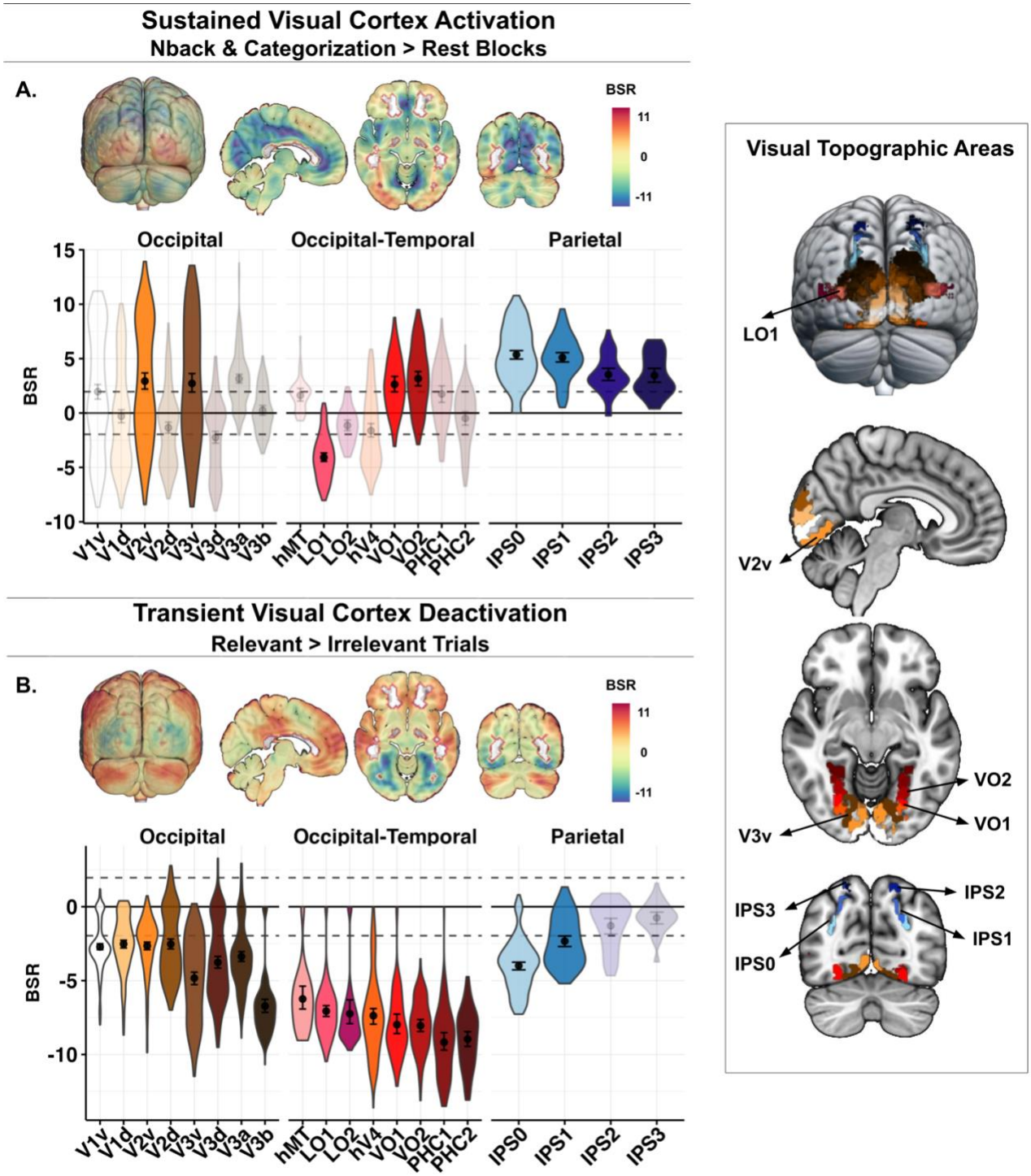

Fig. S3. Sustained and transient task-related activation across visual topographic areas. Panel A shows sustained task > rest block activation patterns (reported in Fig. S2), and Panel B shows transient task-relevant > irrelevant trial activation patterns (reported in Fig. 3). Untresholded whole-brain maps are shown for reference. The mean BSR values (±99% CIs) were computed across voxels within each region of the maximum probability atlas of visual topographic areas from Wang et al. (20), displayed in the panel on the right. The distribution of BSR values across all voxels is also displayed – solid colors indicate statistically significant differences from the BSR threshold of reliability, while transparent colors indicate non-significant differences. Dashed lines denote BSR = ±1.96 (equivalent to p = .05).

Attentional Control and Perceptual-Processing Regions Are Functionally-coupled During Working Memory Maintenance. A prevailing view of top-down control is its reliance on context-dependent functional coupling between lateral frontal control regions and posterior perceptual regions (23). Our results show that coactivation of control and visual networks is not observed when comparing task-relevant versus -irrelevant trials. It is possible, however, that FC between frontal control and category-selective higher-order perceptual regions supported the active working memory maintenance of task-relevant stimuli (24). To test this possibility, we compared FC between the inferior frontal junction (IFJ) control region and the posterior fusiform face area (FFA) and parahippocampal place area (PPA) regions, which are selectively engaged by faces and places, respectively, during the time interval between stimulus display and its N-back match. We reasoned that, if FC between control and perceptual regions supports working memory maintenance, the IFJ would couple with the FFA during face trials but not place trials, and with the PPA during place trials but not face trials. Only N-back trials with correctly detected matches/repeats were included to ensure that the percept was held in working memory.

Regions of interest were defined in each participant using a group-constrained functional localizer approach. The right IFJ was selected based on its greater engagement during the N-back task compared to the Categorization task (Figure 2A). The FFA and PPA were chosen for their preferential activation during face and place N-back blocks, respectively (Figure 2B). Each participant's data were analyzed individually to identify regions of interest in the IFJ (N-back vs Categorization blocks), and in the PPA and FFA (face vs place N-back blocks). Peak BSR coordinates within the group-constrained regions of interest were extracted from each participant's result map. These coordinates served as the centers of 27-voxel cubes, from which the mean BOLD signal change was extracted across relevant N-back trials (note that only repeated trials were included) for each experimental condition of interest (Fame by Domain). Three participants were excluded from the analysis due to having fewer than seven events in at least one condition of interest. The N-back trials were analyzed as events spanning four TRs. To maximize data points per participant, events were not averaged across runs.

We then computed the product-moment correlation between the BOLD timeseries of the IFJ with the PPA and FFA for each experimental condition. The correlation coefficients were Fisher's z-transformed before the statistical analysis, which included 1) ANOVAs to assess the effects of fame and domain, and 2) one-sided one-sample t-tests to assess the presence of FC, with Benjamini-Hochberg correction applied to control the false discovery rate.

As expected, FC between IFJ and PPA was stronger for places compared to faces (Figure S4; $F(1, 26) = 12.55$, $p = 0.002$, pes = 0.33). Notably, IFJ and PPA exhibited positive FC during place trials regardless of fame (Famous Place: $t(26) = 3.75$, $p = 0.007104$, $d = 0.72$; Anonymous Place: $t(26) = 2.9$, $p = 0.0302$, $d = 0.56$), but were not coupled during face trials (Famous Face: $t(26) = 0.79$, $p = 0.4971429$, $d = 0.15$; Anonymous Face: $t(26) = 0.64$, $p = 0.529$, $d = 0.12$). We did not find the expected main effect of working memory for faces on the FC between IFJ and FFA ($F(1, 26) = 0.43$, $p = 0.516$, pes = 0.02). This null effect might be explained by the inconsistent modulation of the FFA by top-down control observed across previous studies (25, 26).

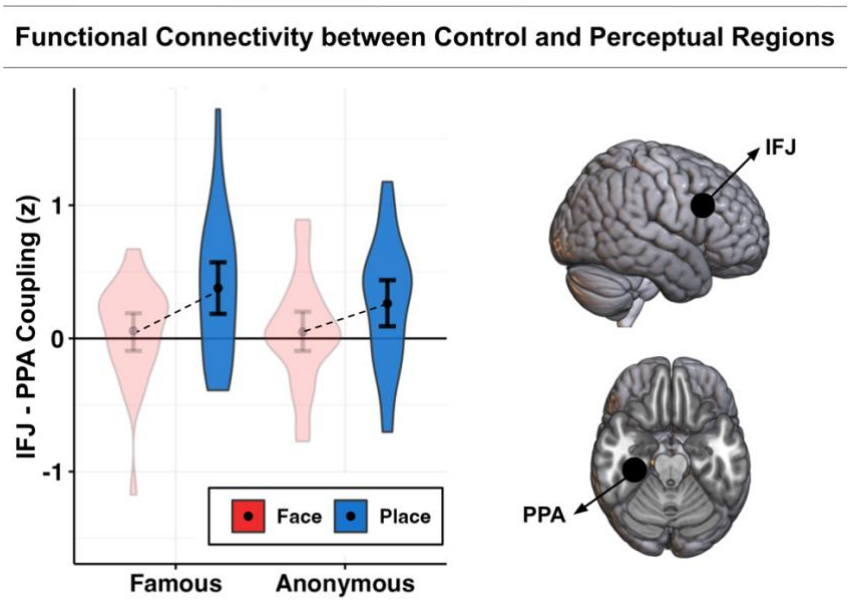

Fig. S4. Functional connectivity between IFJ and PPA as a function of stimulus fame and domain. Mean standardized correlation coefficients (±95% CI) across participants are shown along with the corresponding distributions. Solid colors indicate statistically significant deviations from zero, whereas

transparent colors indicate non-significant effects. Dashed lines between condition means denote statistically significant pairwise differences. The schematic brain image shows the approximate locations of the regions of interest.

Attentional Selection and Non-selective Perceptual Decisions Recruit Opposite Ends of the Principal Gradient. Although the control analysis indicated that categorization trials exhibited an opposite pattern to task-relevant trials, it was unclear whether this pattern would persist independently of the task-irrelevant condition that contributed more strongly to the negative expression of the LV. To test the robustness of the original pattern and whether the categorization trials intrinsically express an opposite pattern to task-relevant trials, we conducted a supplementary PLS analysis including only task-relevant and categorization trials as a function of fame. This analysis revealed a significant whole-brain pattern of neural activity (Figure S5-A) that dissociated task relevant from categorization trials irrespective of stimulus fame (Figure S5-B). This pattern was highly similar to the one observed in the main analysis reported in Figure 3 ($r = 0.924$, $p = 0.001$).

We then computed the spatial correlation between the unthresholded map and the principal gradient map from Margulies et al. (17). This revealed a statistically significant positive correlation between position along the gradient and the strength of neural modulation by attentional selection relative to perceptual categorization ($r = 0.539$, $p = 0.005$). Gradient Bins 9 and 10, representing the heteromodal extreme of the gradient, showed reliably stronger activation for relevant trials. In contrast, Bin 2, located at the unimodal end of the gradient, showed reliably stronger activation for categorization trials. These results suggest that selective working memory and perceptual decisions preferentially recruit opposite ends of the principal gradient.

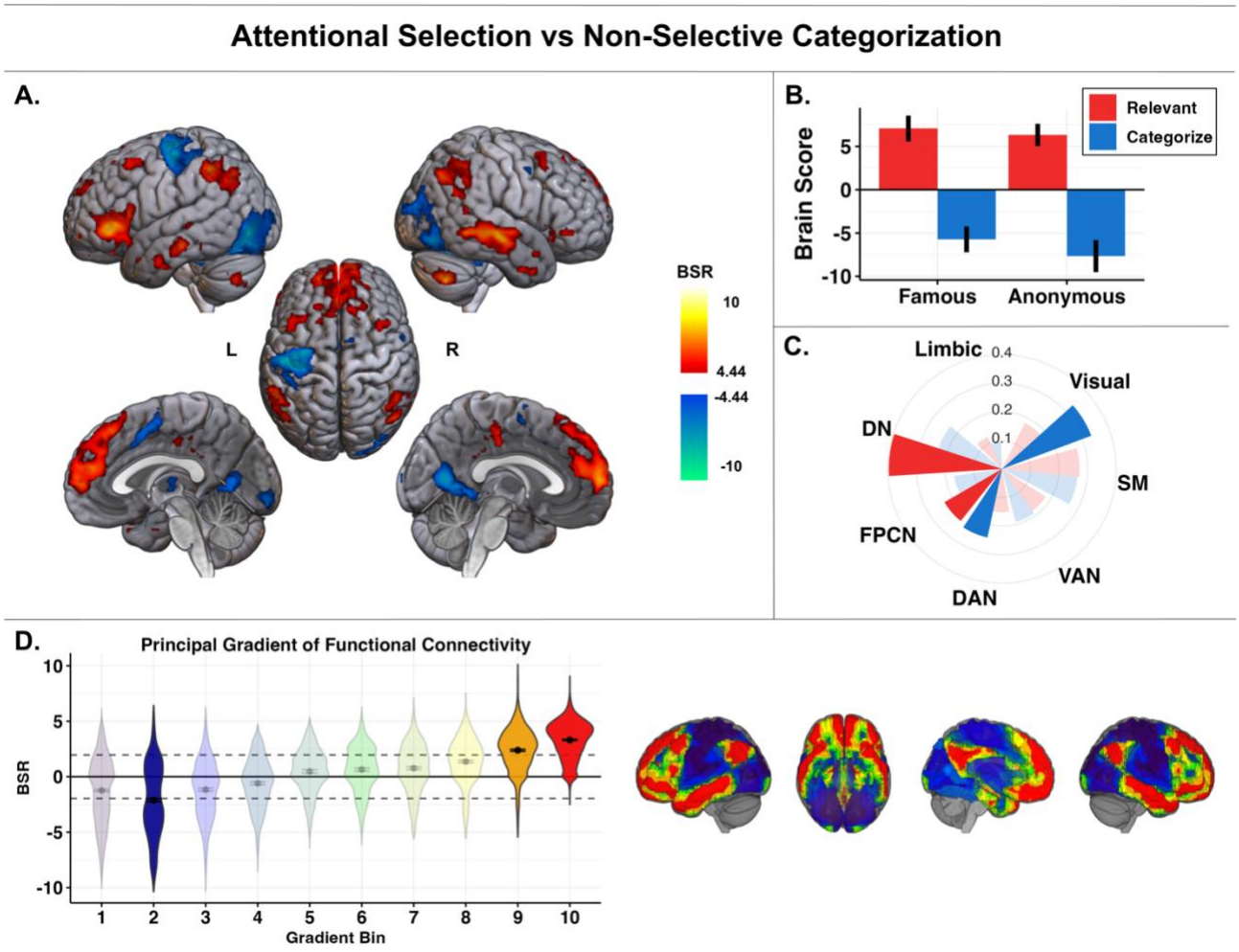

Figure S5. Differences in transient activity in response to relevant versus categorized trials irrespective of fame. Panel A. The maps show the top 5% of voxels based on BSR values (BSR > ± 4.44, equivalent to $p < 8.98e\text{-}06$). Panel B. The mean brain scores (± SD) associated with the statistically significant LV. Panel C. The degree of overlap between the brain pattern associated with the positive (red) and negative (blue) expression of the LV (thresholded at $|BSR| > 1.96$, $p < .05$) and the 7-network parcellation from Yeo et al. (12). Solid colors indicate statistically significant overlap, while transparent colors indicate non-significant overlap. Panel D. The mean BSR scores (± 99% CIs) across the voxels that fall within each bin of the principal gradient from Margulies et al. (17). The distribution of BSR values across all voxels is also displayed – solid colors indicate statistically significant differences from the BSR threshold of reliability (BSR = ± 1.96, equivalent to $p = .05$) indicated by the dashed lines, while transparent colors indicate non-significant differences.

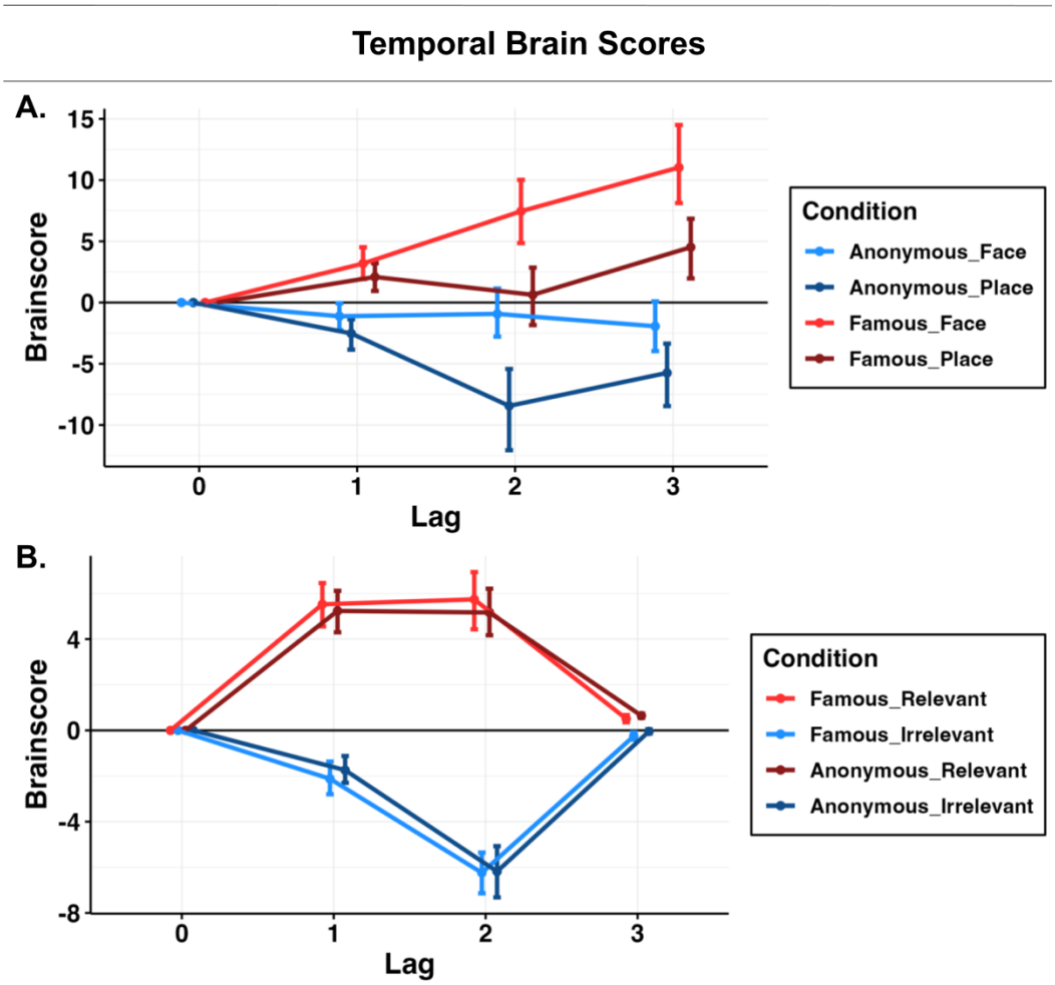

Fig. S6. Temporal Brain Scores. Mean brain scores (±95% CIs) are shown as a function of lag/TR and experimental condition. Panel A. Brain scores from the contrast (rotated) PLS analysis examining the effect of Fame by Domain. Panel B. Brain scores from the non-rotated PLS analysis examining the effects of Task relevance by Fame.

Table S1. Differences in sustained activity during Nback vs Categorization blocks.

Contrast	Region	Peak MNI Coordinates			BSR	Cluster Size
		X	Y	Z		
Nback > Categorization	Insula_R	32.5	22.5	-2.5	9.11	811
	Cingulum_Mid_R	5	22.5	42.5	8.54	3004
	Angular_R	32.5	-62.5	45	7.99	1981
	Fusiform_R	27.5	-42.5	-7.5	7.44	1129
	Insula_L	-30	25	-2.5	6.64	186
	Parietal_Inf_L	-32.5	-52.5	40	5.88	1124
	Frontal_Inf_Tri_L	-50	22.5	30	5.26	654
	Cerebelum_Crus1_L	-10	-72.5	-30	5.20	728
	Cerebelum_Crus2_R	45	-62.5	-47.5	4.84	257
	Fusiform_L	-20	-42.5	-10	4.69	416
	Frontal_Sup_R	25	62.5	10	4.01	396
	Frontal_Inf_Tri_L	-47.5	47.5	12.5	3.81	219
	Calcarine_L	-17.5	-55	7.5	3.57	61
	Frontal_Sup_L	-22.5	57.5	5	3.55	282
	Cerebelum_3_R	7.5	-27.5	-20	3.19	88
Categorization > Nback	Temporal_Sup_L	-40	-15	-5	-5.66	6054
	Cerebelum_8_R	22.5	-62.5	-52.5	-5.64	505
	Precuneus_L	-15	-42.5	65	-5.59	5587
	Insula_R	40	-12.5	-2.5	-5.05	2180
	Cerebelum_Crus1_R	30	-80	-22.5	-4.39	1365
	Cerebelum_Crus1_L	-25	-85	-20	-4.36	492
	Thalamus_L	0	-7.5	-10	-3.97	56
	Temporal_Inf_R	52.5	-2.5	-42.5	-3.72	153
	ParaHippocampal_R	25	15	-30	-3.58	184
	Frontal_Inf_Orb_L	-32.5	45	-15	-3.54	116
	Cerebelum_8_L	-22.5	-65	-57.5	-3.49	258
	Thalamus_L	-10	-20	0	-3.12	54
	Cerebelum_9_L	-12.5	-35	-50	-2.90	54

Table S2. Differences in sustained activity during Face vs Place Nback blocks.

Contrast	Region	Peak MNI Coordinates			BSR	Cluster Size
		X	Y	Z		
Face > Place	Temporal_Inf_R	45	-45	-22.5	8.62	34202
	Occipital_Inf_L	-37.5	-85	-12.5	4.90	755
	Frontal_Mid_L	-47.5	40	30	3.32	789
	Precuneus_L	0	-60	25	3.26	229
Place > Face	Lingual_L	-25	-42.5	-7.5	-11.73	54494
	Frontal_Sup_Orb_R	15	20	-25	-2.18	93

Table S3. Differences in transient activity evoked by Famous compared to Anonymous face/place stimuli.

Contrast	Region	Peak MNI Coordinates			BSR	Cluster Size
		X	Y	Z		
Famous > Anonymous	Temporal_Mid_L	-65	-12.5	-10	6.60	793
	Angular_R	47.5	-65	42.5	4.82	354
	Cerebelum_Crus2_L	-45	-75	-40	4.28	135
	Frontal_Mid_L	-30	40	47.5	4.22	98
	Angular_L	-40	-60	27.5	4.11	533
	Frontal_Sup_Medial_L	-5	37.5	57.5	3.99	64
	Temporal_Pole_Sup_L	-30	12.5	-22.5	3.86	125
	Cingulum_Post_L	-5	-47.5	32.5	3.75	439
	Temporal_Inf_R	47.5	-60	-22.5	3.63	263
	Cerebelum_8_L	-37.5	-50	-60	3.48	133
	Cerebelum_8_R	22.5	-45	-60	3.36	86
	Frontal_Med_Orb_L	-5	47.5	-7.5	3.05	128
Anonymous > Famous	Lingual_R	20	-72.5	-10	-7.45	10601
	Fusiform_R	40	-12.5	-30	-4.66	193
	Supp_Motor_Area_L	-5	0	52.5	-4.48	1237
	Frontal_Mid_R	37.5	-5	57.5	-4.32	295
	Caudate_R	20	22.5	7.5	-4.28	51
	Frontal_Mid_L	-30	40	27.5	-4.14	92
	Frontal_Inf_Orb_R	35	35	-2.5	-4.01	671
	Caudate_L	-10	7.5	-12.5	-3.56	71
	Precentral_L	-27.5	-25	55	-3.25	250
	Frontal_Mid_R	32.5	42.5	37.5	-3.08	70
	Olfactory_R	12.5	5	-15	-3.01	80

Table S4. Differences in the transient activity evoked by Relevant vs Irrelevant famous/anonymous stimuli.

Contrast	Region	Peak MNI Coordinates			BSR	Cluster Size
		X	Y	Z		
Relevant > Irrelevant	Frontal_Sup_Medial_R	10	65	17.5	11.06	22764
	Parietal_Inf_R	55	-47.5	37.5	10.73	9046
	Cerebelum_Crus2_L	-30	-67.5	-40	9.46	2823
	Parietal_Inf_L	-52.5	-47.5	47.5	9.15	4052
	Frontal_Inf_Orb_L	-50	35	-2.5	8.34	772
	Cerebelum_9_L	-5	-45	-47.5	5.94	937
	Cuneus_L	2.5	-87.5	30	3.47	52
Irrelevant > Relevant	Fusiform_L	-35	-57.5	-12.5	-15.89	15124
	Precentral_L	-35	-10	62.5	-7.27	3080
	Pallidum_L	-15	7.5	-2.5	-6.40	431
	Pallidum_R	17.5	7.5	-2.5	-4.75	271
	Insula_R	32.5	22.5	0	-3.90	101

Table S5. Summary statistics from one-tailed one-sample t-tests comparing the BSR of voxels within each Gradient Bin to the reliability threshold (BSR = 1.96).

Bin	t	df	p	Effect Size (Cohen's d)
1 (Unimodal)	-49.15	6,232	1	-0.62
2	-52.95	4,578	1	-0.78
3	-29.07	2,740	1	-0.56
4	-23.68	2,125	1	-0.51
5	-9.91	1,098	1	-0.30
6	-12.11	1,641	1	-0.30
7	-8.86	1,703	1	-0.21
8	1.61	1,974	0.053.	0.04
9	28.71	2,710	<.001***	0.55
10 (Heteromodal)	90.62	5,468	<.001***	1.23

Table S6. Summary statistics from one-tailed one-sample t-tests comparing the BSR of voxels within each extended DN and FPCN sub-network to the reliability threshold (BSR = 1.96).

Network	t	df	p	Effect Size (Cohen's d)
DN-A	84.45	5,135	<.001***	1.18
DN-B	121.30	5,654	<.001***	1.61
DN-C	-49.31	1,312	1	-1.36
FPCN-A	50.10	4,685	<.001***	0.73
FPCN-B	-26.04	3,964	1	-0.41
FPCN-C	-15.71	1,368	1	-0.42
Limbic	15.40	5,654	<.001***	0.20
Temp-Par	59.09	2,083	<.001***	1.29

Table S7. Summary statistics from one-sample t-tests assessing BOLD signal change for selective working memory versus non-selective perceptual categorization trials, examined as a function of task relevance and stimulus fame within the DN, FPCN, and visual networks.

Network	Fame	Task Relevance	t	p	Effect Size (Cohen's d)
DN-A	Anonymous	Irrelevant	-3.12	0.004**	-0.56
	Anonymous	Relevant	4.17	<.001***	0.75
	Famous	Irrelevant	-1.14	0.265	-0.2
	Famous	Relevant	4.57	<.001***	0.82
DN-B	Anonymous	Irrelevant	-2.46	0.0198*	-0.44
	Anonymous	Relevant	3.7	<.001***	0.67
	Famous	Irrelevant	-1.15	0.258	-0.21
	Famous	Relevant	3.27	0.00267**	0.59
DN-C	Anonymous	Irrelevant	2.68	0.012*	0.48
	Anonymous	Relevant	-0.13	0.895	-0.02
	Famous	Irrelevant	2.55	0.0161*	0.46
	Famous	Relevant	-1.89	0.0684	-0.34
FPCN-A	Anonymous	Irrelevant	2.78	0.00928**	0.5
	Anonymous	Relevant	5.03	<.001***	0.9
	Famous	Irrelevant	3.3	0.00252**	0.59
	Famous	Relevant	5.29	<.001***	0.95
FPCN-B	Anonymous	Irrelevant	-2.95	0.00604**	-0.53
	Anonymous	Relevant	0.34	0.733	0.06
	Famous	Irrelevant	0.56	0.581	0.1
	Famous	Relevant	2.81	0.00858**	0.51
FPCN-C	Anonymous	Irrelevant	2.8	0.00884**	0.5
	Anonymous	Relevant	1.77	0.0867	0.32
	Famous	Irrelevant	3.66	<.001***	0.66
	Famous	Relevant	2.15	0.0394*	0.39
Limbic	Anonymous	Irrelevant	-2.18	0.037*	-0.39
	Anonymous	Relevant	1.03	0.311	0.19
	Famous	Irrelevant	-0.81	0.424	-0.15
	Famous	Relevant	0.44	0.665	0.08
Temp-Par	Anonymous	Irrelevant	-4.88	<.001***	-0.88
	Anonymous	Relevant	0.94	0.353	0.17
	Famous	Irrelevant	-2.23	0.0334*	-0.4
	Famous	Relevant	0.67	0.511	0.12
Visual	Anonymous	Irrelevant	4.27	<.001***	0.77
	Anonymous	Relevant	-4.32	<.001***	-0.78
	Famous	Irrelevant	2.15	0.0394*	0.39
	Famous	Relevant	-8.16	<.001***	-1.47

Table S8. The average number of trials per experimental condition across participants for each event-related PLS analysis.

Analysis	Condition	Mean	SD
Fame (by Domain)	Anonymous Face	40	0
	Anonymous Place	40	0
	Famous Face	32.77	4.96
	Famous Place	31.97	4.72
Relevance (by Fame)	Anonymous Irrelevant	31.06	2.24
	Anonymous Relevant	48.45	1.36
	Famous Irrelevant	24.52	3.67
	Famous Relevant	39.94	5.03
Relevance (by Fame and Domain) – Control Analysis I	Anonymous Irrelevant Face	15.90	1.49
	Anonymous Irrelevant Place	15.16	1.44
	Anonymous Relevant Face	24.06	1.26
	Anonymous Relevant Place	24.39	1.43
	Famous Irrelevant Face	12.48	2.86
	Famous Irrelevant Place	12.03	2.63
	Famous Relevant Face	19.84	3.30
	Famous Relevant Place	20.10	3.25
Relevance (by Fame and Task) – Control Analysis II	Anonymous Categorized	28.97	2.66
	Anonymous Irrelevant	31.00	2.24
	Anonymous Relevant	48.29	1.37
	Famous Categorized	22.94	3.01
	Famous Irrelevant	24.87	3.76
	Famous Relevant	39.87	5.14

References

1. W. P. Banks, Signal detection theory and human memory. *Psychological Bulletin* **74**, 81–99 (1970).

2. D. Bates, M. Mächler, B. Bolker, S. Walker, Fitting Linear Mixed-Effects Models Using lme4. *Journal of Statistical Software* **67**, 1–48 (2015).

3. A. Kuznetsova, P. B. Brockhoff, R. H. B. Christensen, lmerTest Package: Tests in Linear Mixed Effects Models. *Journal of Statistical Software* **82**, 1–26 (2017).

4. R. V. Lenth, *et al.*, emmeans: Estimated Marginal Means, aka Least-Squares Means.

5. S. M. Smith, Fast robust automated brain extraction. *Human Brain Mapping* **17**, 143–155 (2002).

6. P. Kundu, *et al.*, Integrated strategy for improving functional connectivity mapping using multiecho fMRI. *Proceedings of the National Academy of Sciences* **110**, 16187–16192 (2013).

7. S. M. Smith, J. M. Brady, SUSAN—A New Approach to Low Level Image Processing. *International Journal of Computer Vision* **23**, 45–78 (1997).

8. A. Krishnan, L. J. Williams, A. R. McIntosh, H. Abdi, Partial Least Squares (PLS) methods for neuroimaging: A tutorial and review. *NeuroImage* **56**, 455–475 (2011).

9. A. R. McIntosh, F. L. Bookstein, J. V. Haxby, C. L. Grady, Spatial Pattern Analysis of Functional Brain Images Using Partial Least Squares. *NeuroImage* **3**, 143–157 (1996).

10. A. R. McIntosh, B. Mišić, Multivariate Statistical Analyses for Neuroimaging Data. *Annual Review of Psychology* **64**, 499–525 (2013).

11. L. Q. Uddin, *et al.*, Controversies and current progress on standardization of large-scale brain network nomenclature. *Network Neuroscience* (2023). https://doi.org/https://doi.org/10.1162/netn_a_00323.

12. B. T. Yeo, *et al.*, The organization of the human cerebral cortex estimated by intrinsic functional connectivity. *Journal of Neurophysiology* **106**, 1125–1165 (2011).

13. L. R. Dice, Measures of the Amount of Ecologic Association Between Species. *Ecology* **26**, 297–302 (1945).

14. R. D. Markello, *et al.*, neuromaps: structural and functional interpretation of brain maps. *Nat Methods* **19**, 1472–1479 (2022).

15. A. Alexander-Bloch, *et al.*, On testing for spatial correspondence between maps of human brain structure and function. *Neuroimage* **178**, 540–551 (2018).

16. J. Wu, *et al.*, Accurate nonlinear mapping between MNI volumetric and FreeSurfer surface coordinate systems. *Human Brain Mapping* **39**, 3793–3808 (2018).

17. D. S. Margulies, *et al.*, Situating the default-mode network along a principal gradient of macroscale cortical organization. *Proceedings of the National Academy of Sciences* **113**, 12574–12579 (2016).

18. M. Girn, R. Setton, G. R. Turner, R. N. Spreng, The “limbic network”, comprising orbitofrontal and anterior temporal cortex, is part of an extended default network: Evidence from multi-echo fMRI. *Network Neuroscience* 1–40 (2024). https://doi.org/10.1162/netn_a_00385.

19. A. Kassambara, rstatix: Pipe-Friendly Framework for Basic Statistical Tests. (2023). Deposited 1 February 2023.

20. L. Wang, R. E. B. Mruczek, M. J. Arcaro, S. Kastner, Probabilistic Maps of Visual Topography in Human Cortex. *Cereb Cortex* **25**, 3911–3931 (2015).

21. A. Chamma, *et al.*, nilearn. (2025). https://doi.org/10.5281/zenodo.17043133. Deposited 3 September 2025.

22. K. C. R. Fox, R. N. Spreng, M. Ellamil, J. R. Andrews-Hanna, K. Christoff, The wandering brain: Meta-analysis of functional neuroimaging studies of mind-wandering and related spontaneous thought processes. *NeuroImage* **111**, 611–621 (2015).

23. C. D. Gilbert, W. Li, Top-down influences on visual processing. *Nat Rev Neurosci* **14**, 350–363 (2013).

24. A. Gazzaley, A. C. Nobre, Top-down modulation: bridging selective attention and working memory. *Trends in Cognitive Sciences* **16**, 129–135 (2012).

25. A. Gazzaley, J. W. Cooney, K. McEvoy, R. T. Knight, M. D'Esposito, Top-down Enhancement and Suppression of the Magnitude and Speed of Neural Activity. *Journal of Cognitive Neuroscience* **17**, 507–517 (2005).

26. J. Z. Chadick, A. Gazzaley, Differential coupling of visual cortex with default or frontal-parietal network based on goals. *Nat Neurosci* **14**, 830–832 (2011).